Electronic Supplementary Material (ESI) for ChemComm.
This journal is © The Royal Society of Chemistry 2021

Supporting Information

Optochemical control of transcription by the use of 7-deaza-adenosine-based diarylethenes

Simon M. Büllmann†, Theresa Kolmar†, Philip Slawetzky, Simon Wald and Andres Jäschke*

Institute of Pharmacy and Molecular Biotechnology, Heidelberg University, Im Neuenheimer Feld 364, Heidelberg, 69120, Germany

General Information

Synthesis and purification

Commercially available reagents were purchased from Sigma Aldrich, Carbolution and Carbosynth. These reagents and laboratory grade solvents were used without further purification. Dry solvents were purchased in sealed bottles over molecular sieves. Solvents for oxygen-sensitive reactions were degassed prior use by a continuous argon flow through the reaction mixture for about 10 minutes. All reactions were monitored by TLC (thin layer chromatography) using coated silica plates with fluorescent indicator and visualized with UV-light (254 nm) or stained with a blue-shift solution ($Ce(SO_4)_2$; molybdatophosphoric acid; sulfuric acid). Reactions under high pressure were conducted in microwave tubes sealed with a gas tight climber cap. Flash chromatography was performed according to Still et al.[1] with silica gel 60 (0.04-0.063 mm) using laboratory grade solvents.

Analytics

High-resolution mass spectra were recorded on a Bruker microTOF-Q II ESI (ESI). NMR-spectra were recorded on Varian Systems 300 and 500 instruments. The chemical shifts (δ) are indicated in parts per million (ppm) downfield of TMS and referenced to the respective residual undeuterated solvent peak as follows: $CDCl_3$= 7.26 ppm; DMSO-d_6= 2.50 ppm; MeOH-d_4= 3.31 ppm for ^{1}H-NMR and $CDCl_3$= 77.0 ppm; DMSO-d_6= 39.4 ppm; MeOH-d4= 49.00 ppm for ^{13}C-NMR. Apparent coupling constants (J) are reported in Hz. HPLC measurements were performed using an Agilent 1100 Series HPLC system equipped with a multi-wavelength detector (MWD). A C18 column from VDS optilab (VDSpher Pur 100 C18-H, 250*4.6 mm, 5 µM) was used with a flow rate of 1 mL/min and eluting with a gradient of water and acetonitrile or buffer A and B (buffer A = 100 mM triethylammonium acetate in water, buffer B = 100 mM triethylammonium acetate in 80% acetonitrile).

Determination of the Hammett parameter σ'

The Hammett parameters of the substituents linked by a benzene ring to the thiophene component were determined by ^{13}C carbon NMR spectroscopy according to a literature procedure.[2] The chemical shift of the carbon atom in para to the substitution (C4) divided by that of a carbon atom in benzene was used as the Hammett parameter σ':

$$\sigma' = \frac{^{13}C\ shift\ of\ C4}{^{13}C\ shift\ of\ C\ in\ benzene}$$

Determination of the photochromic properties

For measuring the absorbance spectra of the nucleosides, 2 mL of a 60 µM solution of the sample in water/ethanol (2/1) was prepared and added to a quartz cuvette from Hellma (Model: 110-10-40, Macro). For the oligonucleotides, 400 µL of a 40-50 µM solution of the sample in TRIS buffer (40 mM Tris-HCl, pH 7, 22 mM $MgCl_2$) was added to a quartz cuvette from Starna (Model: 28-F-Q). After the irradiation of the sample with a UV-light LED (310 nm LED: Thorlabs, Mounted High Power LED, operated at 350 mA) at defined time points, an absorbance spectrum was recorded with a Cary 100 Bio UV/VIS-spectrometer from Varian and the data was analyzed with the software CaryWinUV and OriginPro 9.1.

Determination of the thermal stability

For the determination of the thermal stability, 2 mL of a 60 µM solution of the sample in water/ethanol (2/1) or DMSO was prepared and added to a quartz glass cuvette from Hellma (Model: 110-10-40, Macro). For the oligonucleotides 400 µL of a 40-50 µM solution of the sample in TRIS buffer (40 mM Tris-HCl, pH 7, 22 mM $MgCl_2$) was added to a quartz cuvette from Starna (Model: 28-F-Q). Irradiation of the sample was performed with an UV-light LED (310 nm LED: Thorlabs, Mounted High Power LED, operated at 350 mA) until the photostationary state (PSS^{UV}) was reached. Then the absorption maximum at ~ 500 nm of the closed-ring isomer was recorded over 60 min at 40°C, 50°C, 60°C and 70°C for the nucleoside and at 37°C for the oligonucleotides with a Cary 100 Bio UV/VIS-spectrometer from Varian. The recorded data was evaluated with the software Cary Win UV and OriginPro 9.1. Data processing included baseline correction and plotting the absorbance at ~ 500 nm of the closed isomer at a time t (A), divided by the absorption measured at the beginning of the measurement (Ao) versus time. The thermal half-lives were calculated by fitting the normalized absorbance at ~ 500 nm with a 1^{st} order exponential decay equation from OriginPro 9.1.

Determination of the reversibility

For the determination of the fatigue resistance, 2 mL of a 60 µM solution of the sample in water/ethanol (2/1) were prepared and added to a quartz cuvette from Hellma (Model: 110-10-40, Macro). For the oligonucleotides 400 µL of a 40-50 µM solution of the sample in TRIS buffer (40 mM Tris-HCl, pH 7, 22 mM $MgCl_2$) was added to a quartz cuvette from Starna (Model: 28-F-Q). Then the solution was irradiated with an UV-light LED (310 nm LED: Thorlabs, Mounted High Power LED, operated at 350 mA) until the photostationary state (PSS^{UV}) was reached and an absorption spectrum was recorded with a Cary 100 Bio UV/VIS-spectrometer from Varian. Afterwards the sample was irradiated with visible light (490 nm LED: Thorlabs, Mounted High Power LED, operated at 350 mA) until the absorption band in the

visible wavelength range was erased, and a spectrum was recorded. This process was repeated for ten cycles and the absorption maximum in the visible wavelength range of the closed-ring isomer was normalized to 1 and plotted.

Determination of the switching efficiency

For the determination of the switching efficiency, HPLC measurements were performed using an Agilent 1100 Series HPLC system equipped with a multi-wavelength detector (MWD). A C18 column from VDS optilab (VDSpher Pur 100 C18-H, 250*4.6 mm, 5 µM) was used with a flow rate of 1.0 mL/min and eluting with a gradient of buffer A and B (buffer A = 100 mM triethylammonium acetate in water, buffer B = 100 mM triethylammonium acetate in 80% acetonitrile). The absorbance was recorded at the isosbestic wavelength of the open and closed isomers of the photoswitch. The gradients used for the determination of the photostationary states (PSS^{UV}) and the isosbestic wavelengths are summarized in Table S1. The switching efficiency was then determined by calculating the ratio of the peak areas of the open and closed isomer at the isosbestic point. Peaks that could not be separated completely on the HPLC were separated with the peak analyzer of origin pro 2015.

Table S1: HPLC-gradients used for the determination of the photostationary states (PSS^{UV}) and the isosbestic wavelengths of the corresponding compound.

	$PhNH_2$	PhOMe	Np	Ph	2Py	$Ph(CF_3)_2$	Ph^{t}Bu	Pym	Oligos
Gradient [% of B]	40-70	50-90	50-90	50-90	40-70	60-90	60-90	40-70	20-50
Isosbestic wavelength [nm]	322	318	228	320	336	335	297	336	280

Determination of the cyclization and cycloreversion quantum yields[3,4]

Quantum yields were measured on an updated Quantum yield determination setup (QYDS) by Megerle et al.[3] Irradiation of the photoswitches was performed, using UV-light LEDs (Nikkiso SMD mounted 300 nm LED, model: VPC173) and visible light LED (Osram Oslon SSL80 505 nm LED, model: LVCK7P-JYKZ). The LED output radiant power was calibrated against the output voltage of the solar cell by using a power meter from Coherent (model: PowerMax-USB PS19Q). The raw data measured with the QYDS was further processed with a Mathcad script provided by the Riedle group. The calculation of the quantum yields is based on the "initial slope method". Therefore, the power of the LED was turned down sufficiently enough that the formation of the product is linear. Data processing with the Mathcad script includes baseline correction, spectral decomposition of each spectrum into the substrate and product base spectrum, and calculation of the quantum yields by the number of incoming photons per

second and wavelength. Conversion to the cyclization product was calculated using the extinction coefficients of both isomers. Hereby, the concentration changes of the two isomers are numerically simulated with account to the spectral dependencies of molar absorptivities and LED light. The spectral composition of the PSS^{UV} is a linear combination of the open- and closed-isomer, which makes it possible to calculate the spectrum of pure closed isomer, if the composition of the PSS^{UV} is known. The composition of the PSS^{UV} was determined as described earlier, by separation of both isomers on an analytical HPLC column and subsequent integration of the peaks at an isosbestic point. The spectrum of pure closed isomer can be calculated using the following equation, where X represents the portion of open form and Y the portion of closed form in the photostationary state (PSS^{UV}):

$$E_{CF} = \frac{(E_{PSS} - E_{OF})\,X}{Y}$$

During the measurement, a "shutter file" is generated which displays the exact irradiation time points as well as the absorbed radiant power of each step. The shutter files of the fully characterized photoswitchable nucleosides are shown in the appendix.

Synthesis and purification of photochromic oligonucleotides

The modified oligonucleotides were synthesized using solid-phase phosphoramidite chemistry with an automated oligonucleotide synthesizer (H6, V.01.02, K&A Laborgeraete Gbr) in the 5'-DMT-off mode. Reagents were purchased from Roth and Sigma Aldrich (Proligo) and used without further purification. As solid support, 500 Å CPG (Controlled Pore Glass) was used. DNA standard phosphoramidites were dissolved in dry acetonitrile with a concentration of 0.05 M. The modified phosphoramidites were dissolved in dry acetonitrile with a concentration of 0.07 M. A standard 1 µmol DNA protocol was used. After the synthesis, the solid phase was treated with 25% aqueous ammonia (4 h, 40°C) and washed three times with Millipore water (1 mL) to extract the oligonucleotide completely from the solid support. The ammonia/water mixture was lyophilized, the crude product dissolved in water, filtered and purified by HPLC using a semi-preparative Luna C18 column (5 µm, 250 x 15.0 mm, Phenomenex) with a flow rate of 6 mL/min. As solvents, gradients (0 min – 20 min, 10% - 22% B, 20 min- 21 min, 22% - 35% B, 21 min – 40 min, 35% - 55% B) of buffer A and buffer B (buffer A = 100 mM triethylammonium acetate in water, buffer B = 100 mM triethylammonium acetate in 80% acetonitrile) were used. The manually collected product fractions were lyophilized twice and the residual oligonucleotide was dissolved in 0.5 mL Millipore water. The concentration was determined on a Nanodrop One (Thermo Fischer Scientific) and the aqueous stock solutions were stored at – 21°C.

Measurement of melting curves[5]

Melting temperatures were determined for functionalized DNA duplexes prepared by annealing a synthetic natural single strand purchased from Integrated DNA Technologies (IDT) and oligonucleotides prepared by solid-phase phosphoramidite chemistry. DNA duplexes containing no modified nucleotides, served as control. The final concentration of double stranded DNA for T_m measurement was 1 µM in 400 µl phosphate buffer (10 mM, 0.1 M NaCl pH 7). Thermal denaturation studies were performed in triplicate on a Cary 100 Bio UV/Visible spectrometer with temperature controller (Varian). Melting temperatures (Tm values in °C) were obtained by plotting temperature versus normalized absorbance, applying a differential curve fit.

Photoregulation of *in vitro* transcription

The sense and antisense ssDNA template strands (unmodified ssDNA: each 100 µM, from IDT, Table S2) were mixed in an equimolar ratio, incubated for 5 min at 95°C before snap cooling on ice. A master mix containing in vitro transcription buffer (IVT buffer: 40 mM Tris-HCl, pH 8, 1 mM spermidine, 22 mM $MgCl_2$, 0.01% Triton X-100), 2 mM nucleoside triphosphates (NTPs), 10 µM malachite green (MG) or TMR-DN, 10 mM dithiothreitol (DTT), pyrophosphatase (PPase), T7-RNA-polymerase (T7-RNAP) and water was prepared (Table S3). The closed form (CF) of the DNA template was generated by irradiation with 340 nm UV light from the top in an Eppendorf tube. The in vitro transcription was performed in a 30 µL scale using a 384 well-plate format (UV-permeable from Greiner, UV-Star). Time course measurements of fluorescence intensity were conducted using a Tecan Sapphire 2 fluorescence microplate reader (Tecan Group Ltd., Männedorf, Switzerland). The following settings were applied for fluorescence measurements: high sensitivity mode, lambda exc/em: 635/655 nm for MG and 564/590 nm for TMR-DN; 8 nm excitation/emission bandwidth; measurement position: bottom of the well plate; gain 90-120; measurement every 8 s; at 37°C. All in vitro transcriptions were performed in triplicates and the obtained data were analyzed with Origin Pro 2015.

Table S2: Sequences of DNA strands used for in vitro transcriptions. The DNA strands were purchased from Integrated DNA Technologies, München, Deutschland and used without further purification.

	Sequence (5' - 3')
Fwd-T7	TCT AAT ACG ACT CAC TAT A
Rev-T7	TAT AGT GAG TCG TAT TAG A
Rev-T7-MG	GGA TCC ATT CGT TAC CTG GCT CTC GCC AGT CGG GAT CCT ATA GTG AGT CGT ATT AGA
Rev-T7-RhoBAST	GGA ACC TCC GCG AAA GCG GTG AAG GAG AGG CGC AAG GTT AAC CGC CTC AGG TTC CGG AAC CTC CGC GAA AGC GGT GAA GGA GAG GCG CAA GGT TAA CCG CCT CAG GTT CCT ATA GTG AGT CGT ATT AGA

Table S3: Pipetting scheme for a (15x) master mix using 30 µL per reaction and a DNA template concentration of 250 nM. ATP: adenosine triphosphate, GTP: guanosine triphosphate, CTP: cytosine triphosphate, UTP: uridine triphosphate, MG: malachite green (stock in DMSO), DTT: dithiothreitol, Ppase: pyrophosphatase, T7-RNAP: T7-RNA polymerase.

Volume	**Substance**	**Stock [c]**	**Final [c]**
45 µL	IVT-buffer (10x)	10x	1x
18 µL	ATP	50 mM	2 mM
18 µL	GTP	50 mM	2 mM
18 µL	CTP	50 mM	2 mM
18 µL	UTP	50 mM	2 mM
22.5 µL	DTT	200 mM	10 mM
22.5 µL	MG/TMR-DN	200 µM	10 µM
22.5 µL	Ppase	0.1 U/µL	0.001 U/µL
22.5 µL	T7-RNAP	1 mg/mL	0.05 mg/mL
202.5 µL	H2O	/	/
(15x) 1.5 µL	Template (+,-,OF,CF)	5 µM	250 nM

Supporting Figures

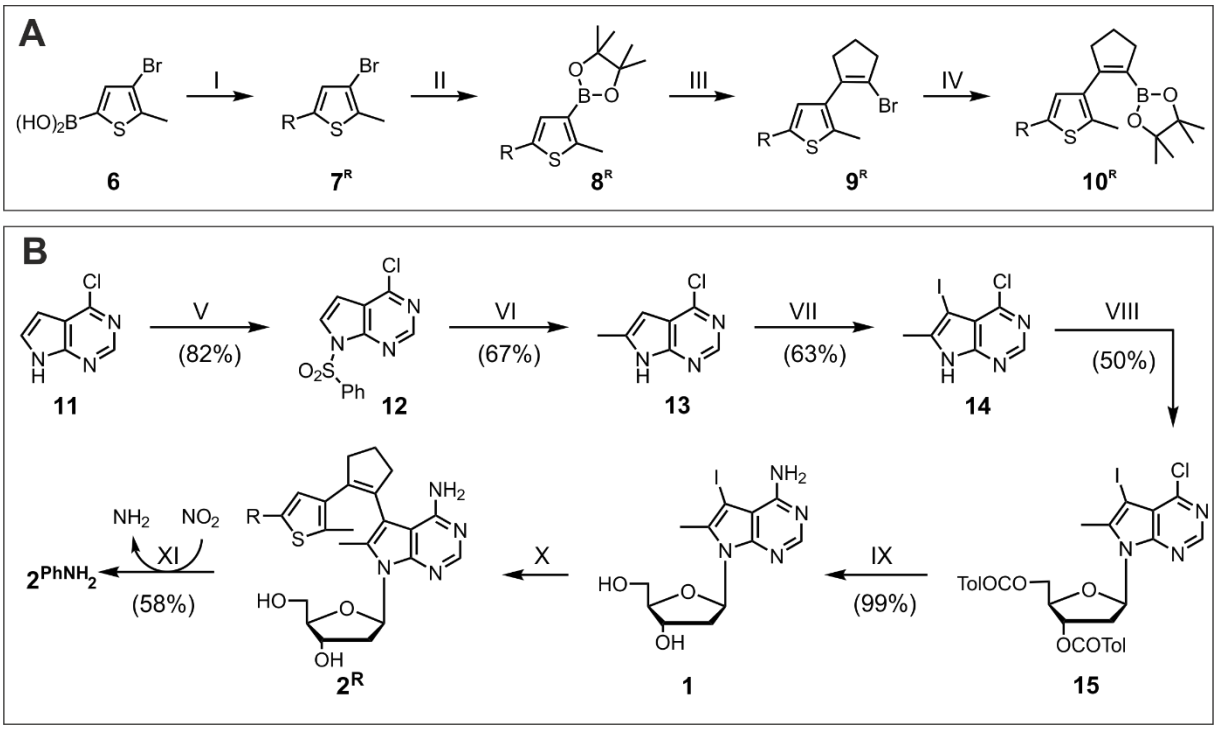

Figure S1 Synthetic overview for the preparation of 7-deaza-adenosine bases photochromic DAEs. (A) Optimized route for the synthesis of the pinacolate ester building blocks **(10^{R})**, that was used for the residues: $PhNO_2$, $Ph(CF_3)_2$ and Pym. (I) Ar-X, Na_2CO_3 (aq.), $Pd(dppf)Cl_2$, 80°C, THF; (II) Bis(pinacolato)diboron, KOAc, XPhos, $Pd(PPh_3)_4$, 120°C, dioxane; (III) Dibromocyclopentene, Cs_2CO_3, $Pd(PPh_3)_2Cl_2$, 80°C, DMF; (IV) Bis(pinacolato)diboron, KOAc, XPhos, $Pd(PPh_3)_4$, 120°C, dioxane The other pinacolate ester building blocks were synthesized according to literature procedures.[6] (B) Synthesis of the 7-deaza-adenosine building block **(1)** and final Suzuki coupling with the pinacolate ester building blocks **(10^{R})**. (V) NaH, benzenesulfonyl chloride, 0°C, THF; (VI) n-BuLi, TEMEDA, MeI, -78°C, THF; (VII) KO^{t}Bu, 0°C, THF; (VIII) N-Iodosuccinimide, rt, DCM; i) KOH, TDA-1, Hoffer's chlorosugar, rt, DCM; (IX) NH_3 (aq.), 150°C, 150 W, 20 bar, microwave; (X) pinacolate ester **(10^{R})**, Na_2CO_3, $Pd(PPh_3)_4$, 80°C, DME/H2O (2/1); (Xl) Reduced iron powder, rt, EtOH/AcOH (2/1), sonicator.

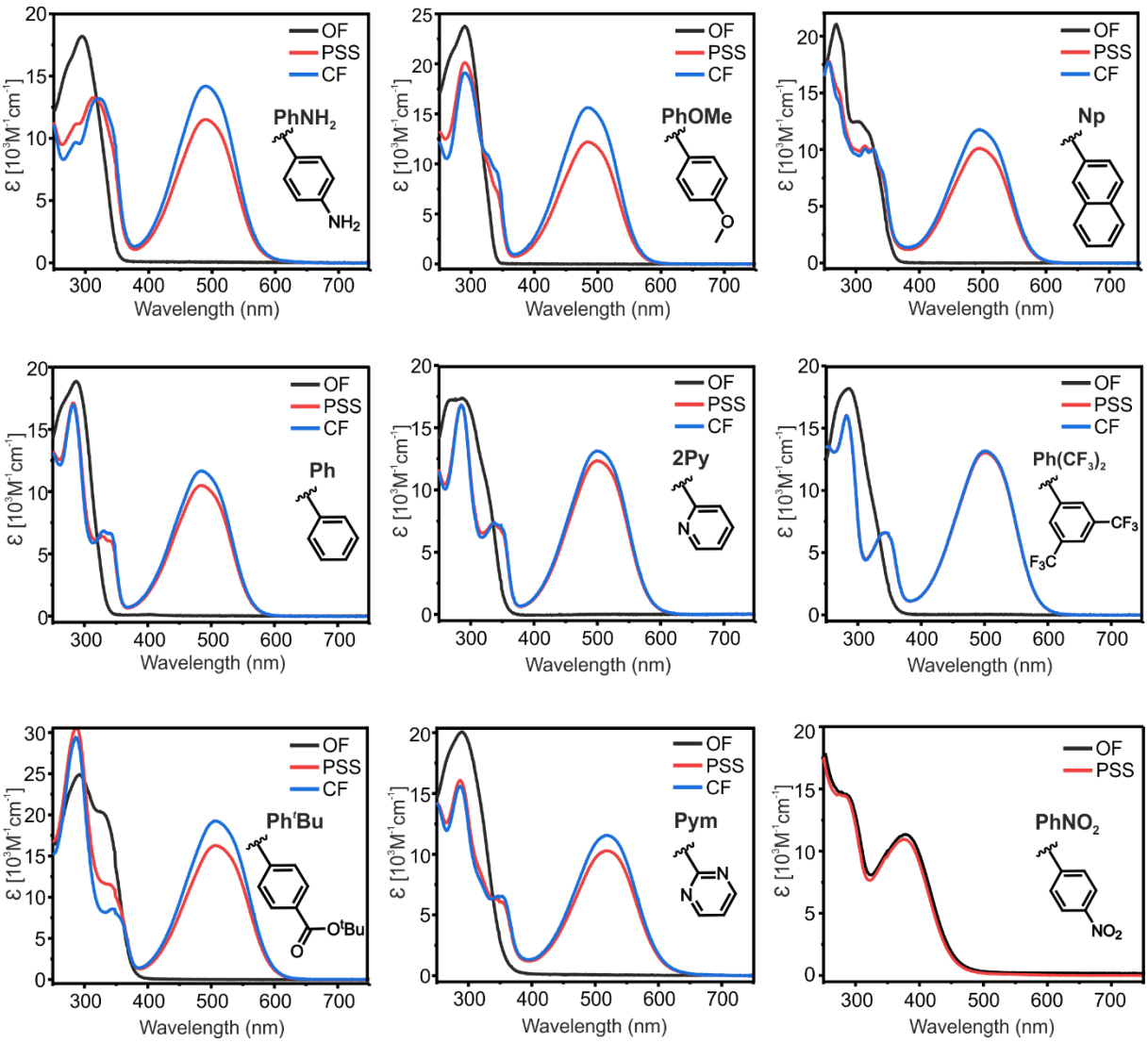

Figure S2: Absorption spectra of 7-deaza-adenosine-based photoswitches. A 60 µM solution of the compound in a water/ethanol mixture (2/1) was prepared and a UV/Vis spectrum was recorded (black line). Irradiation with UV light led to the formation of the PSS^{UV} and a UV/Vis spectrum was recorded (red line). The determined switching efficiencies were used to calculate the spectrum of the pure closed-ring isomer (blue line).

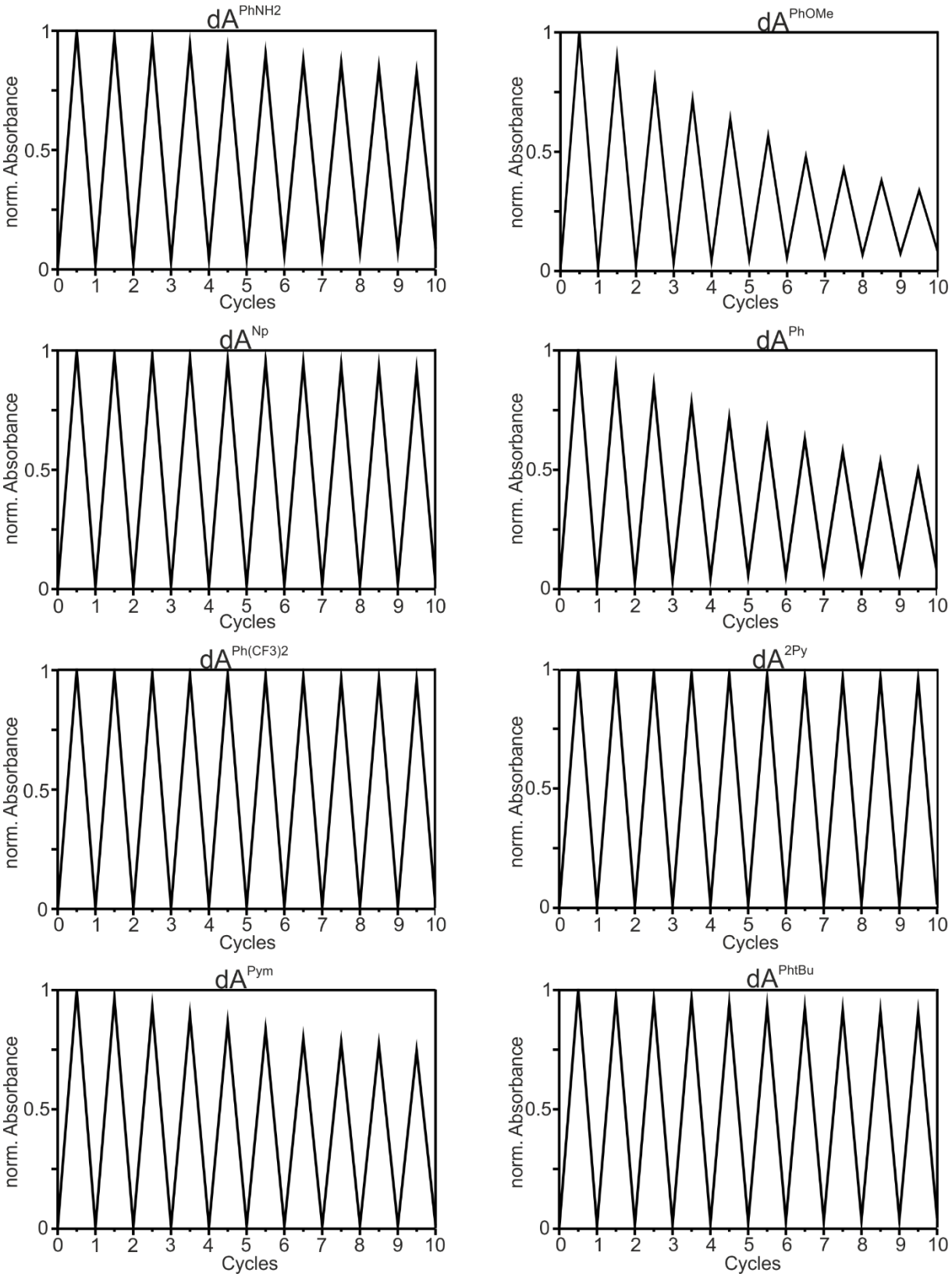

Figure S3: Reversibility of 7-deaza-adenosine-based photoswitches. A 60 µM solution of the compound in a water/ethanol mixture (2/1) was irradiated with UV light until the PSS^{UV} was reached. After recording the UV/Vis spectrum, the solution was irradiated with visible light. This procedure was repeated 10 times.

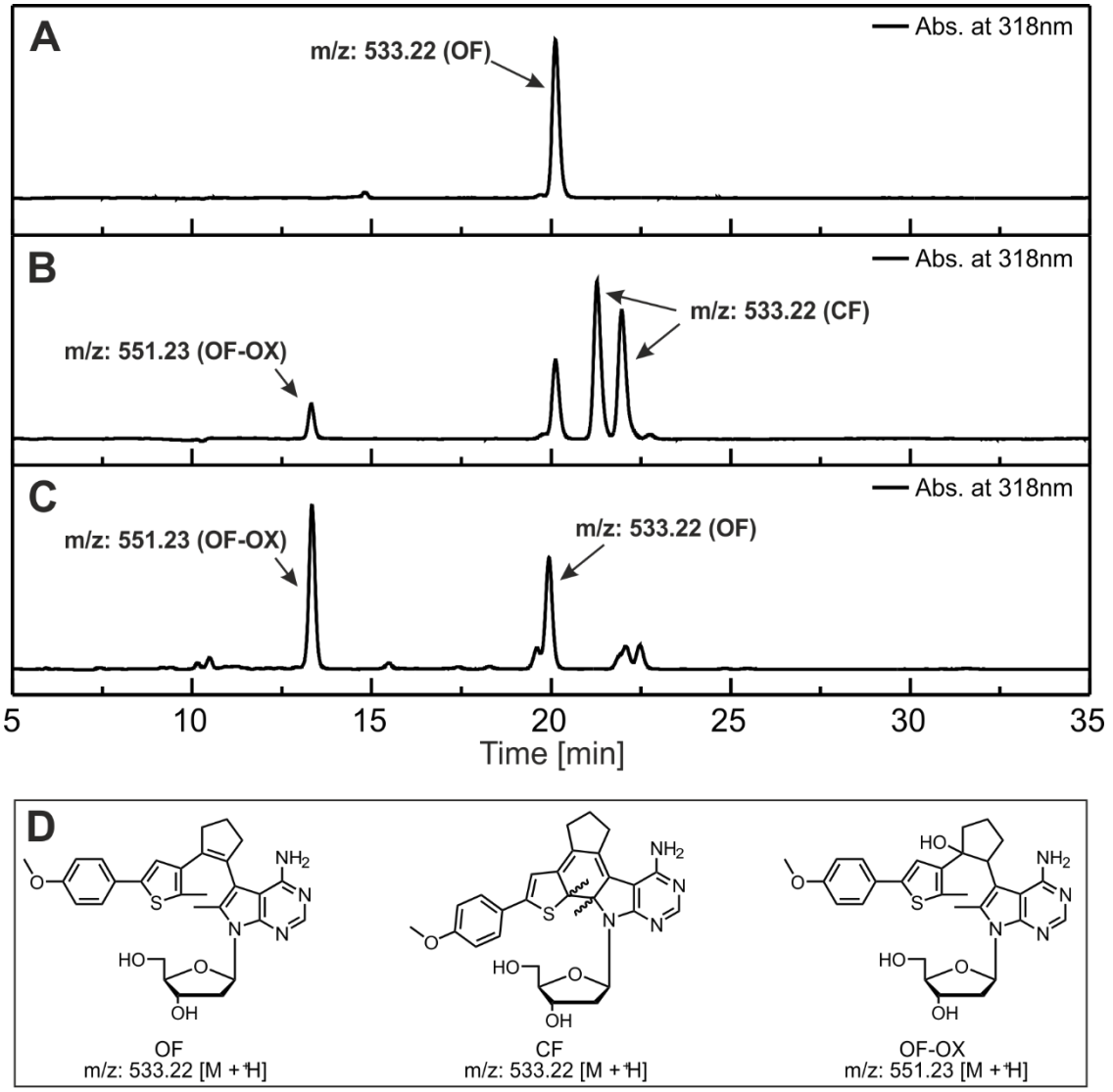

Figure S4: HPLC/MS-based fatigue measurement of dA^{PhOMe}. (A) HPLC trace of the pure open isomer before irradiation with UV light. The displayed peak was collected and analyzed by mass spectrometry (MS). (B) HPLC trace of the PSS^{UV}. The two new peaks at longer retention times were identified as the two diastereomers of the closed isomer. The new peak at shorter retention time was analyzed by MS and could be identified as an oxidation product (hydration). (C) HPLC trace after 10 cycles of back and forth switching. The oxidation product is now the most intensive peak. (D) Structures revealed by MS.

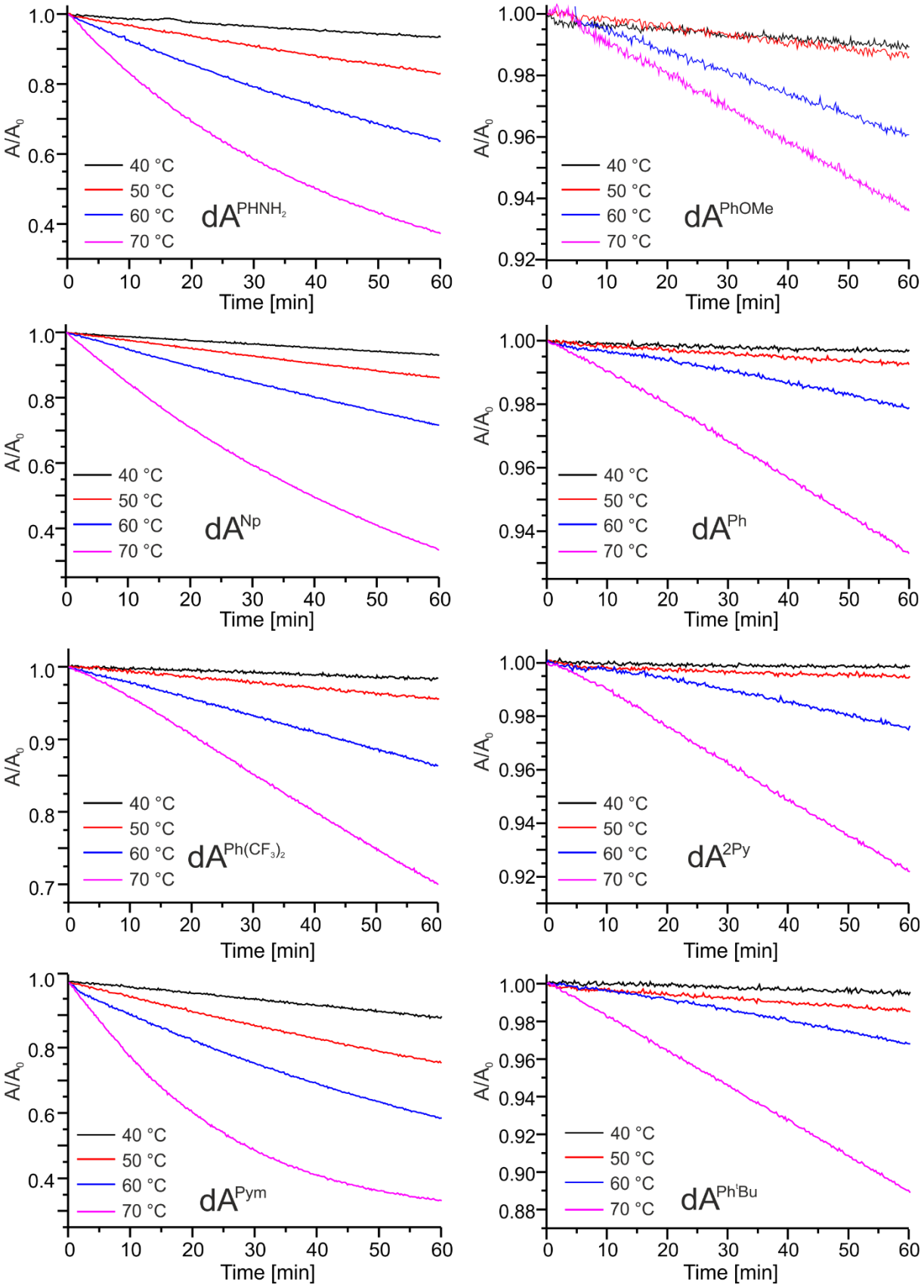

Figure S5: Thermal stability of 7-deaza-adenosine-based photoswitches. A 60 µM solution of the compound in a water/ethanol mixture (2/1) was irradiated with UV light until the PSS^{UV} was reached. After that, the absorption of $\lambda_{max,vis}$ of the closed-ring isomer was measured over 1h.

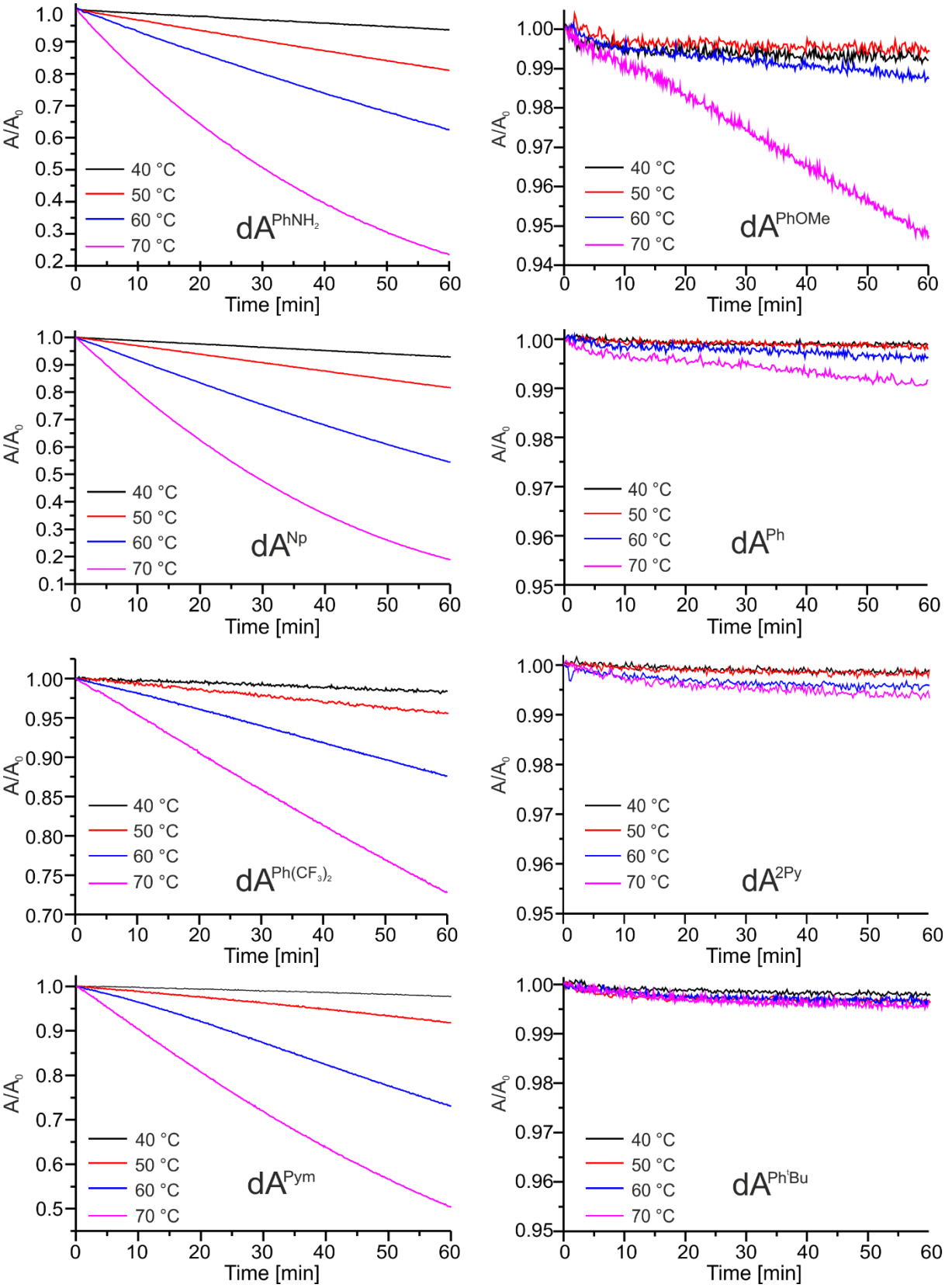

Figure S6: Thermal stability measurements of 7-deaza-adenosine-based photoswitches. A 60 µM solution of the compound in DMSO was irradiated with UV light until the PSS^{UV} was reached. After that the absorption of $\lambda_{max,vis}$ of the closed-ring isomer was measured over 1h.

Table S4: Thermal half lives for the 7-deaza-adenosine photoswitches in water/ethanol (2/1) and DMSO at different temperature.

H_2O/EtOH	dA^{PhNH_2}	dA^{PhOMe}	dA^{Np}	dA^{Ph}	dA^{2Py}	$dA^{Ph(CF_3)_2}$	dA^{Ph^tBu}	dA^{Pym}
$\tau_{1/2}$ [h] (40°C)	10.8	83	9.9	232	256	40	119	5.9
$\tau_{1/2}$ [h] (50°C)	3.3	48	4.6	99	151	15.6	53	2.4
$\tau_{1/2}$ [h] (60°C)	1.6	16.5	2.1	33	27.5	4.7	20.8	1.3
$\tau_{1/2}$ [h] (70°C)	0.7	10.2	0.6	9.9	8.3	1.9	5.9	0.5

DMSO	dA^{PhNH_2}	dA^{PhOMe}	dA^{Np}	dA^{Ph}	dA^{2Py}	$dA^{Ph(CF_3)_2}$	dA^{Ph^tBu}	dA^{Pym}
$\tau_{1/2}$ [h] (40°C)	10.8	228	9.3	431	387	32.7	368	29.5
$\tau_{1/2}$ [h] (50°C)	3.3	170	3.4	290	251	14.3	334	8.2
$\tau_{1/2}$ [h] (60°C)	1.5	68	1.2	214	169	5.2	184	2.2
$\tau_{1/2}$ [h] (70°C)	0.5	13	0.4	97	105	2.2	132	1.0

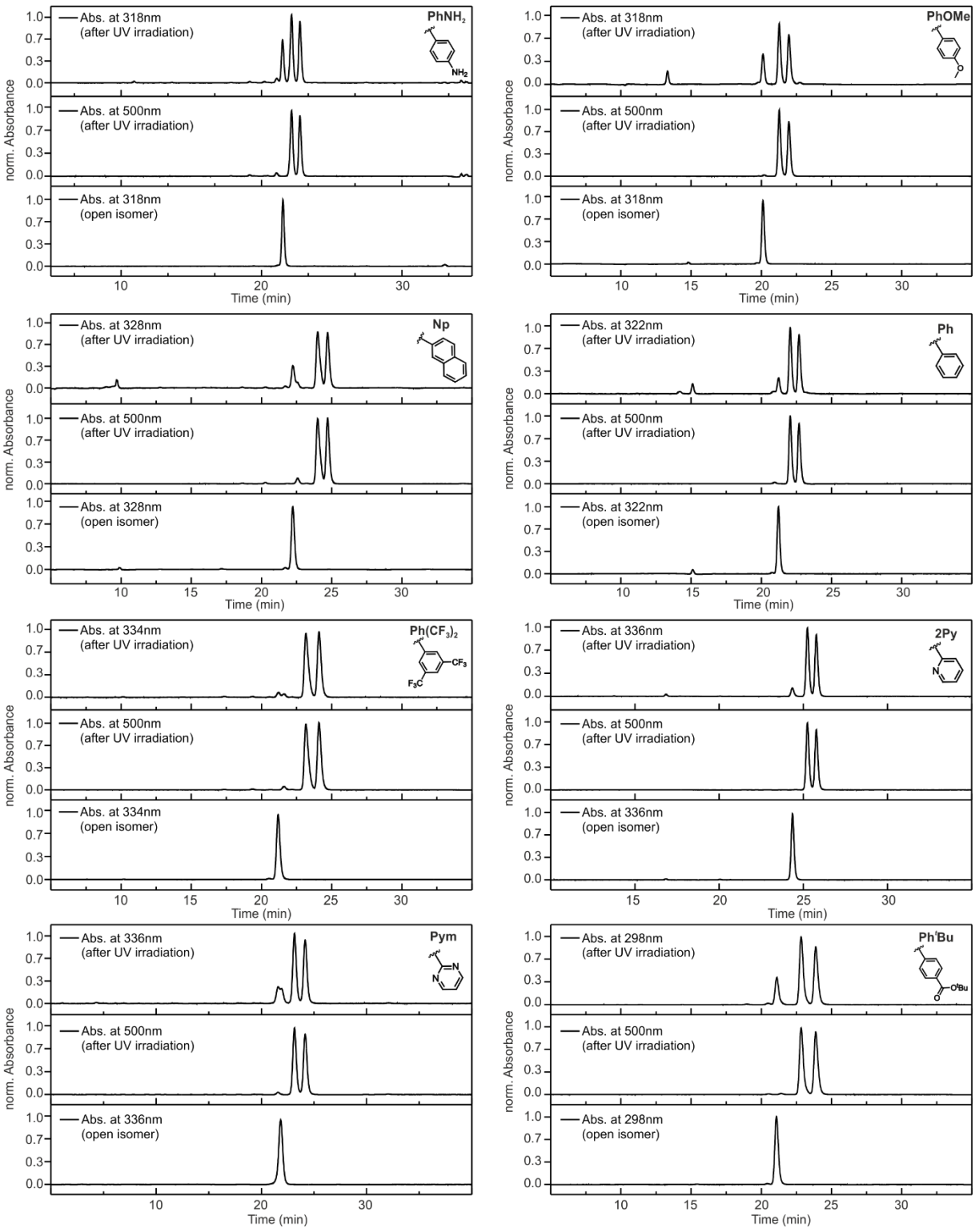

Figure S7: Determination of the switching efficiency of photochromic 7-deaza-adenosine DAEs. The substituent on position 5 of the thiophene moiety is depicted in the upper right corner of each measurement.

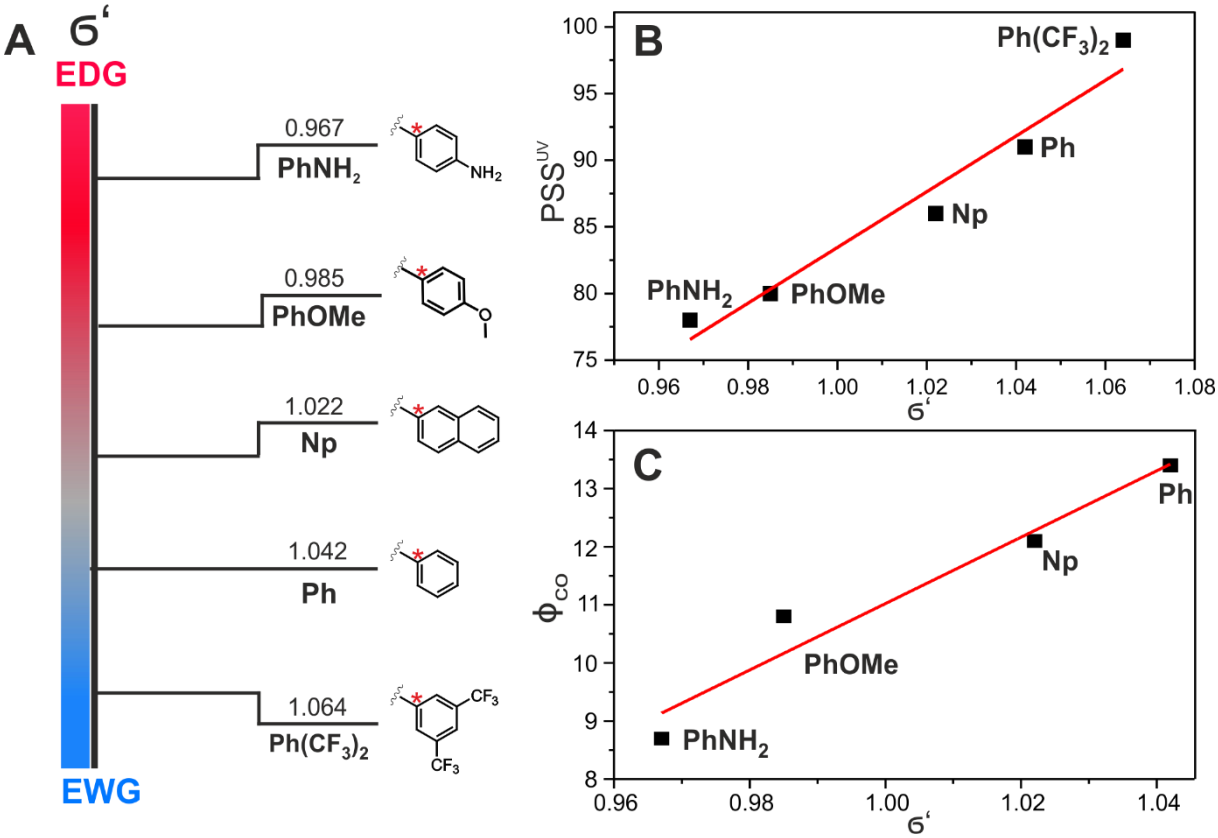

Figure S8: Dependence of selected photophysical properties on the electronic character of the substituents of the 7-deaza-adenosine switches. (Modified) Hammett parameters ϭ‘ were obtained from ^{13}C shifts of carbon C4 (red asterisk).[2] On this scale, a value of ϭ‘ > 1 implies an electron-withdrawing character of the substituent, while ϭ‘ < 1 indicates an electron-donating character. (A) Schematic arrangement of the substituents according to their ^{13}C-derived Hammett parameters (σ’) for derivatives that can be analyzed by this formalism. The carbon atom C4, which was used for the determination of σ’ is marked with a red star. (B) Hammett correlation of σ’ with the PSS^{UV}. (C) Hammett correlation of σ’ with the ring-opening quantum yields.

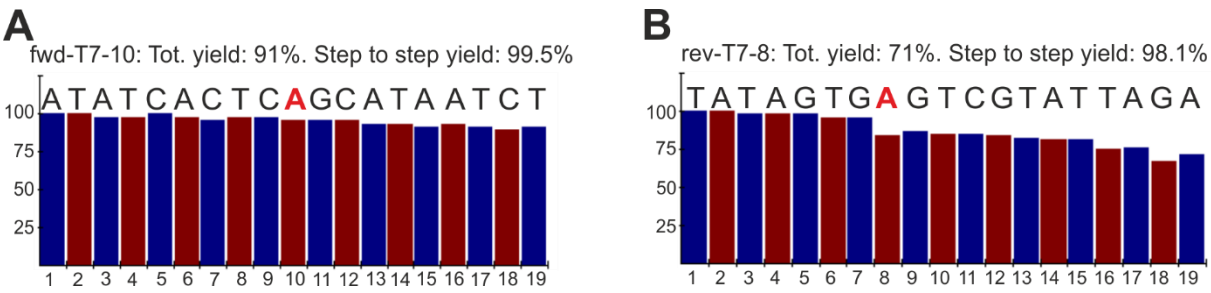

Figure S9: Incorporation of **5**$^{Ph(CF_3)_2}$ into an oligonucleotide with the sequence of the templating and non-templating T7-promotor via solid phase synthesis. (A) Trityl histogram recorded by the oligosynthesizer. The photoswitchable phosphoramidite was incorporated at position -10 (marked in red) of the non-template strand, with high efficiency (see total yield and step to step yield). (B) Trityl histogram recorded by the oligosynthesizer. The photoswitchable phosphoramidite was incorporated at position -8 (marked in red) of the template strand, with high efficiency (see total yield and step to step yield).

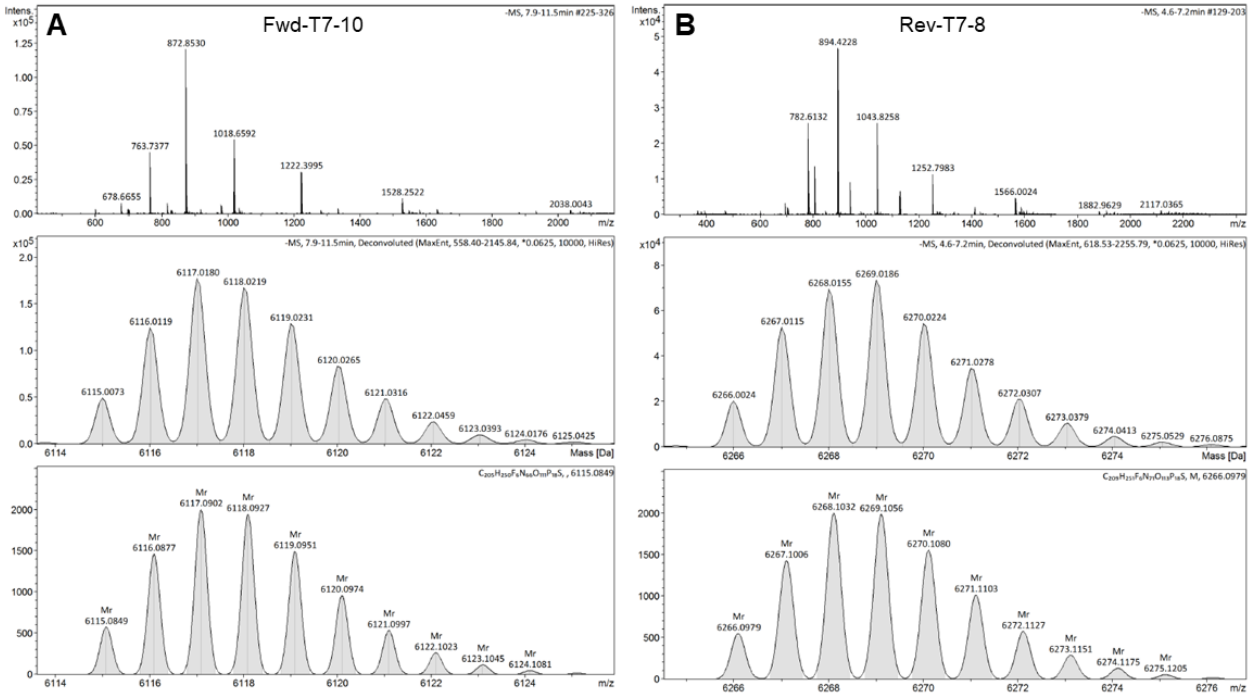

Figure S10: Identification of the modified oligonucleotides via mass spectrometry (ESI, negative mode). (A) MS-data of Fwd-T7-10. (B) MS-data of Rev-T7-8.

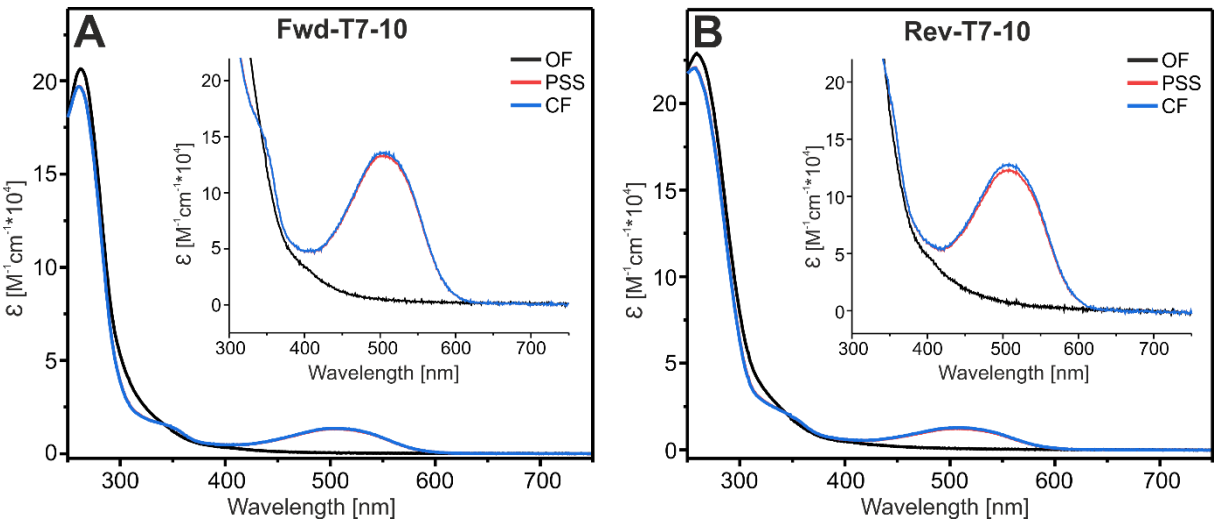

Figure S11: Absorption spectra of the photochromic oligonucleotides. (A) non-template strand (Fwd-T7-10) (B) template strand (Rev-T7-8). The absorption spectra of the open form (black line), photostationary state after UV irradiation (PSS^{UV}, red line) and calculated closed form (blue line) are shown.

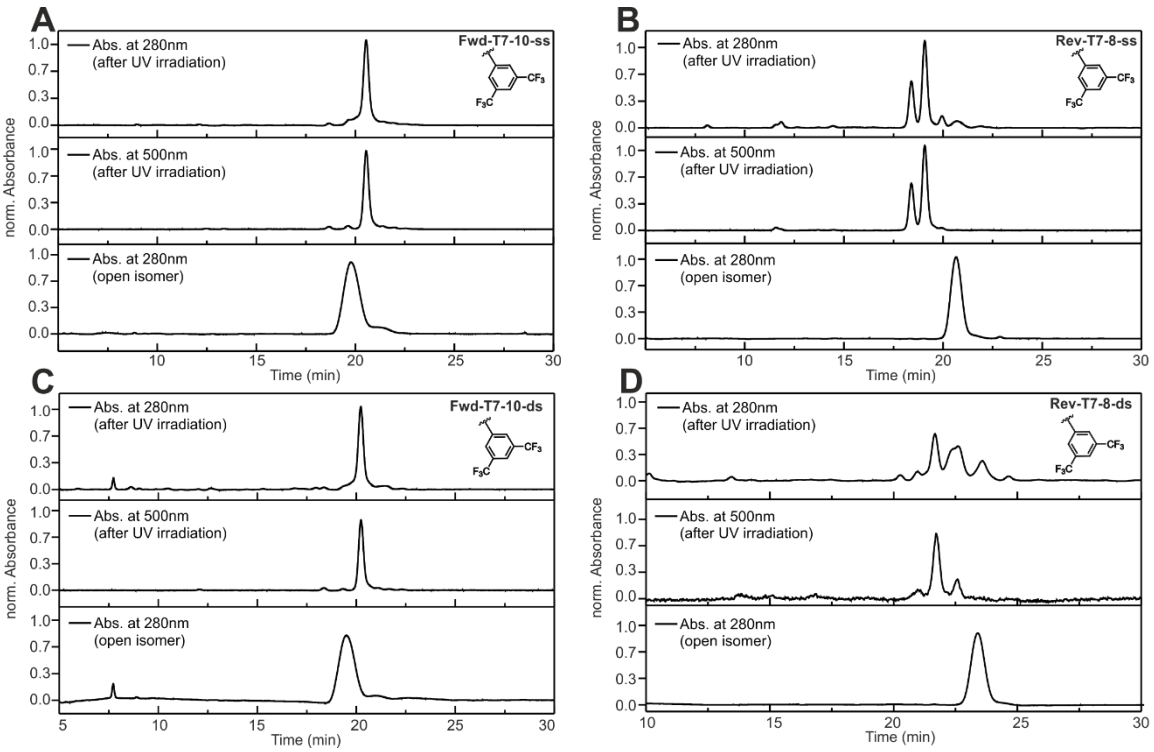

Figure S12: Determination of the switching efficiency of the photochromic oligonucleotides. (A) HPLC traces of Fwd-T7-10 as a single strand. (B) HPLC traces of Rev-T7-8 as a single strand. (C) HPLC traces of Fwd-T7-10 as a duplex. (D) HPLC traces of Rev-T7-8 as a duplex.

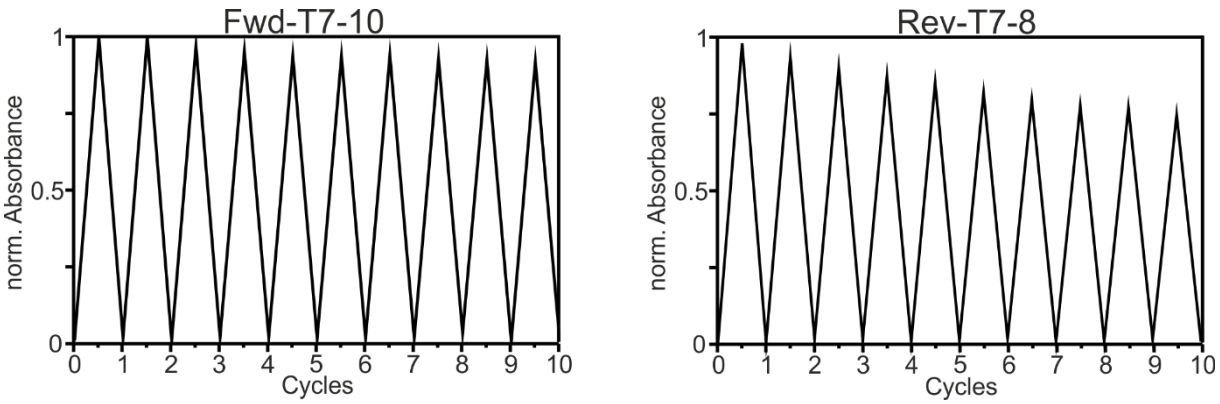

Figure S13: Reversibility measurements of the photochromic oligonucleotides. A 40-50 µM solution of the sample in TRIS buffer was irradiated with UV light until the PSS^{UV} was reached. After recording the UV/Vis spectrum, the solution was irradiated with visible light. This procedure was repeated 10 times.

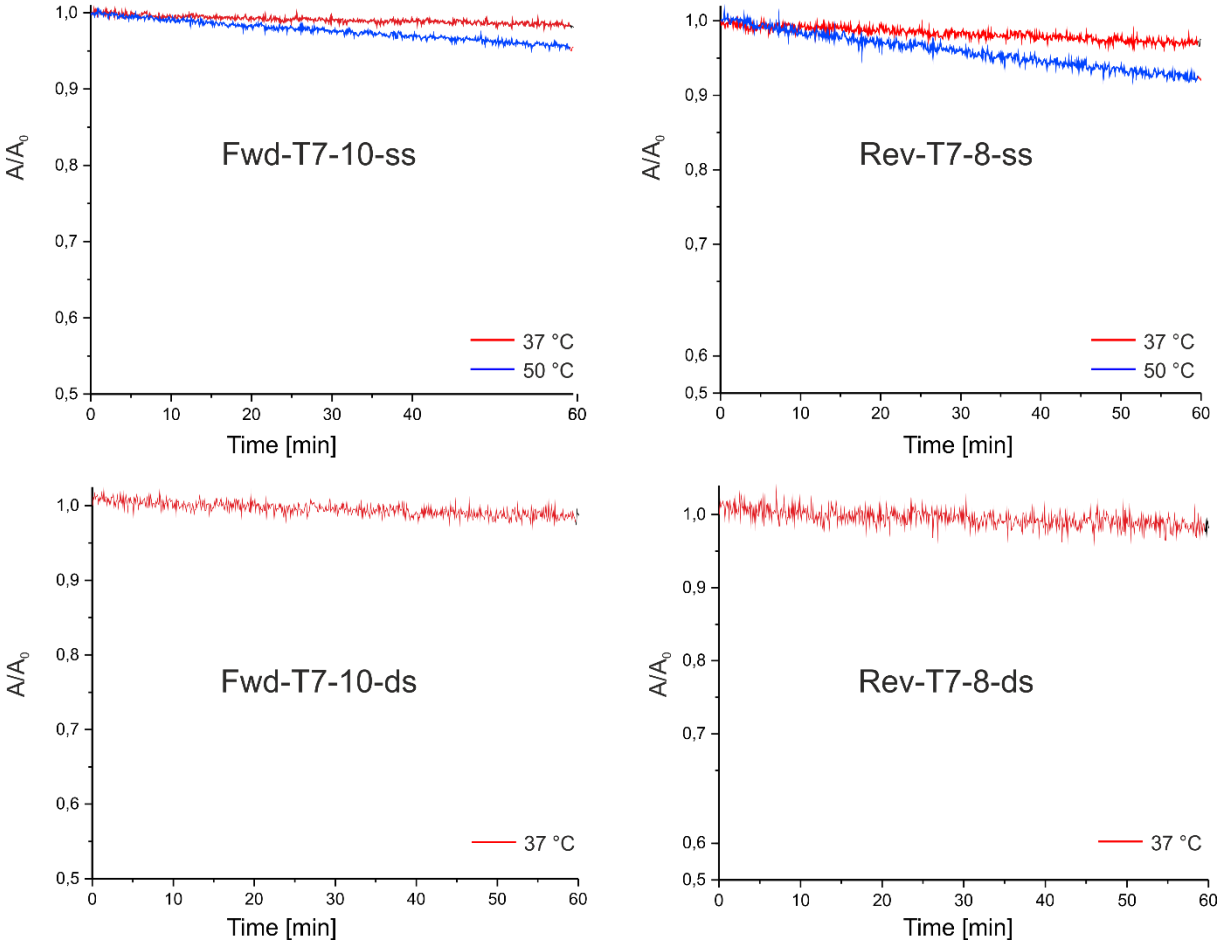

Figure S14 Thermal stability measurements of photochromic oligonucleotides in the single strand (ss) and duplex (ds). A 40 µM solution of the compound in TRIS buffer (40 mM Tris-HCl, pH 7, 22 mM $MgCl_2$) was irradiated with UV light until the PSS^{UV} was reached. After that the absorption of $\lambda_{max,vis}$ of the closed-ring isomer was measured over 1h.

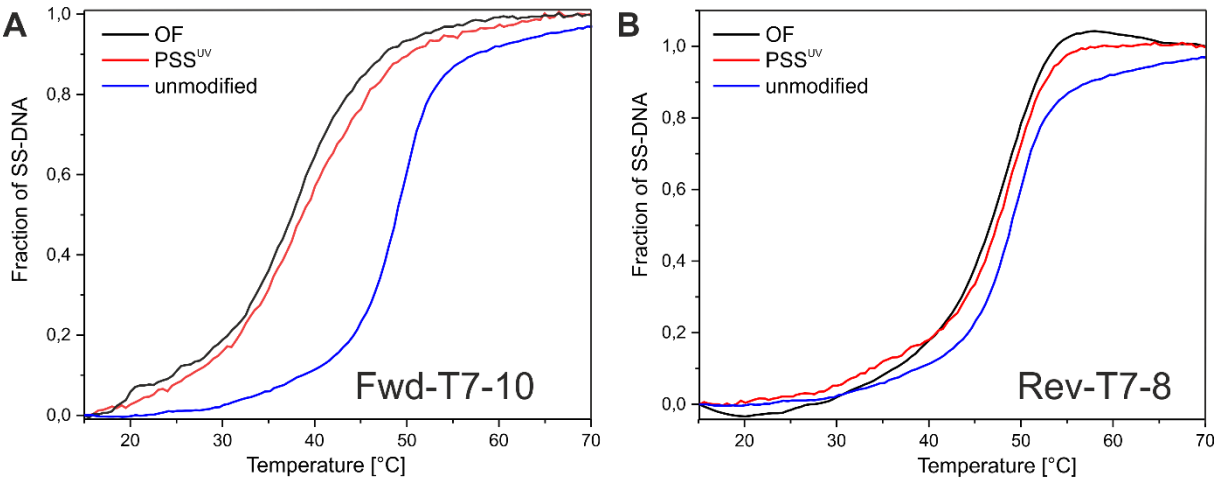

	$T_{M,OF}$	$T_{M,PSS}$	$T_{M,(+)}$
Fwd-T7-10 (ds)	37.75	38.69	/
T7-(+)	/	/	49.05

	$T_{M,OF}$	$T_{M,PSS}$	$T_{M,(+)}$
Rev-T7-8 (ds)	48.52	48.25	/
T7-(+)	/	/	49.05

Figure S15 Melting curves for the modified promotors: (A) Fwd-T7-10 (ds) (B) Rev-T7-8 (ds). Melting curves in its open form (black) and at the PSS^{UV} (red) as well as for the unmodified promotor (blue) are shown.

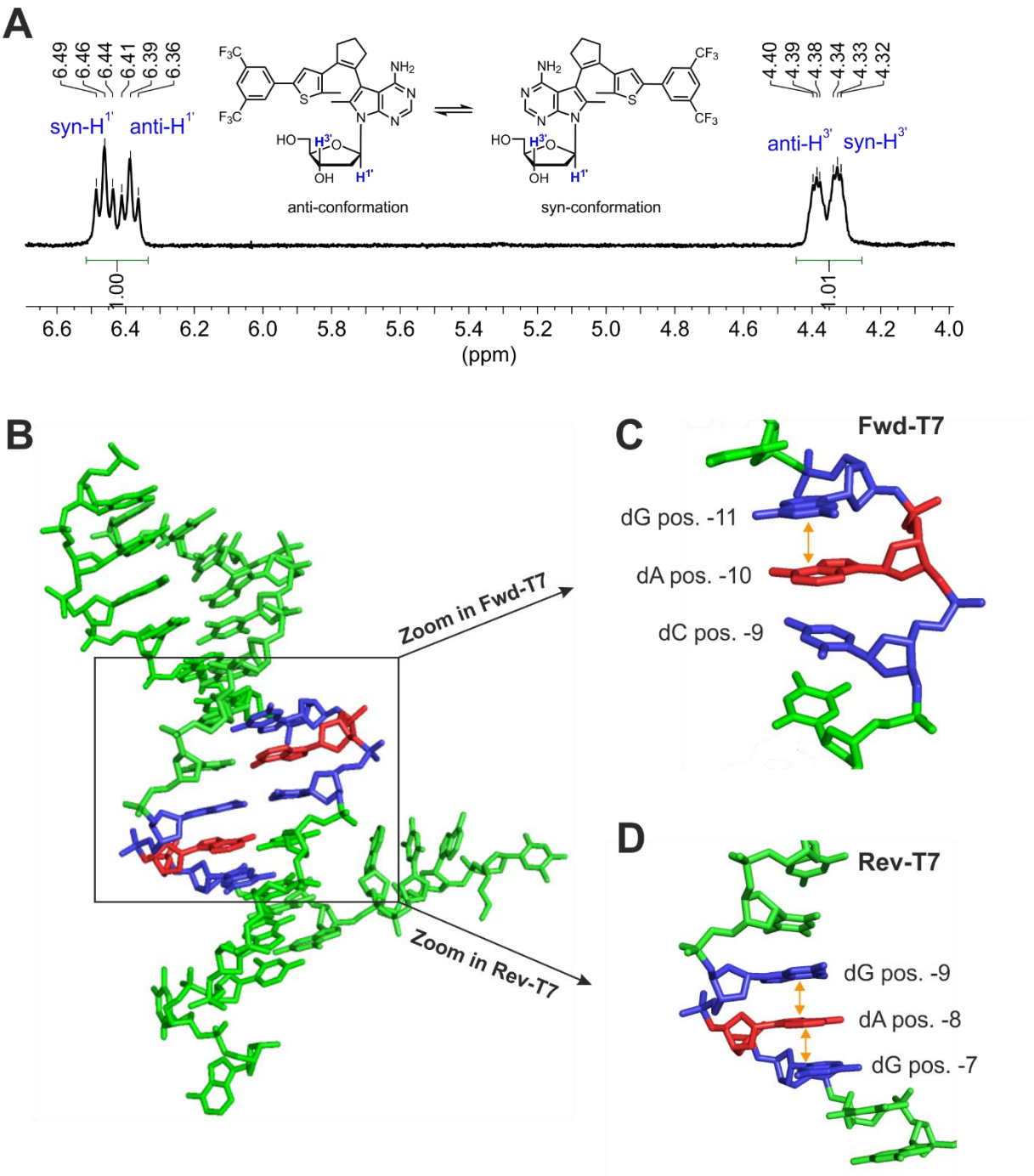

Figure S16 (A) Schematic illustration of Syn- and Anti-conformations of $dA^{Ph(CF_3)_2}$ and the corresponding NMR spectra that shows a set of two signals for the glycosidic proton ($H^{1'}$) and the proton at carbon C3 ($H^{3'}$), which is due to the existence of the two conformations. (B) Crystal structure of the duplex promotor sequence bound to the T7 polymerase adapted from Cheetham et al. (ref). (C) Zoom in of the Fwd-T7 strand (non-template strand) illustrating the environment of the position dA-10 (highlighted in red). (D) Zoom in of the Rev-T7 strand (template strand) illustrating the environment of the position dA-8 (highlighted in red). Stacking interactions between the neighbouring nucleobases are indicated with an orange arrow.

Further Information: We were surprised by the very different behaviour of Fwd-T7 and Rev-T7 apparent in the T_m measurements. We suggest that the neighbouring nucleobases of the photoswitchable purine are in part responsible for this behaviour. Additionally, NMR experiments indicate that the nucleobase of the 7-deaza-adenosine DAEs can occupy both syn- and anti-conformation in relation to the sugar, which was also described for 8-methyl-adenosine derivatives by Dudycz et al.[7] In our case, two sets of signals were apparent for the protons of the deoxy-ribose moiety, revealing the existence of two conformers (45/55 anti/syn). Normally, adenosine is mainly found to be in the anti-conformation. However, the additional methyl group at the reactive alpha carbon atom at the purine DAE and the sterically demanding thiophene moiety lead to the formation of a mixture of the syn- and anti-conformation. In the syn-conformation the alpha methyl group as well as the thiophene moiety are orientated away from the deoxy-ribose. In the duplex, this ratio seems to be dependent on the neighbouring bases. If the photoswitch is surrounded by two G's, the "natural" anti-conformation seems to be stabilized by stacking interactions which promotes base pairing (high melting temperature, Rev-T7-8). On the other hand, if the photoswitch is not stabilized by two G's, the syn-conformation of the purine DEA predominates, therefore inhibiting the formation of base pairing at this position in the duplex (low melting temperature, Fwd-T7-10).

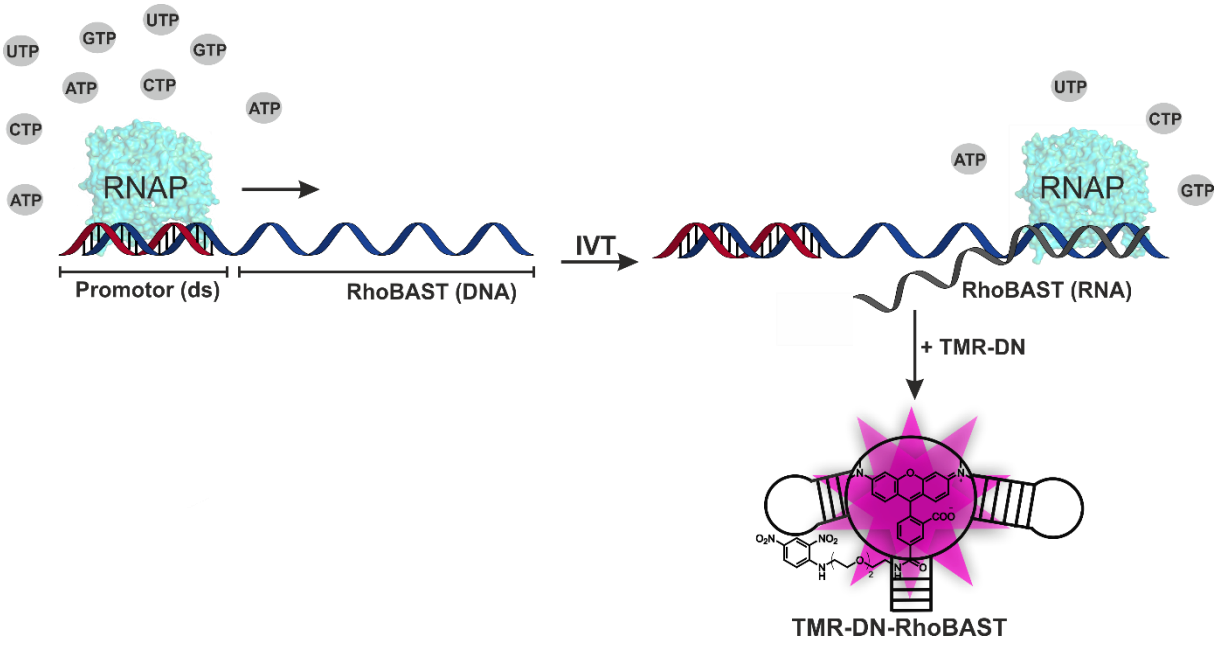

Figure S17: Schematic illustration of the transcription assay with real-time read out. The RNA-polymerase (RNAP) binds to its promotor sequence and the transcription starts. During the transcription the DNA-template strand with the RhoBAST sequence is transcribed to the RhoBAST RNA-aptamer and by the addition of TMR-DN a fluorescence increase could be observed. Our photoswitch is incorporated in the promotor region either in the template strand (blue) at position -8 or in the non-template (red) at position -10.

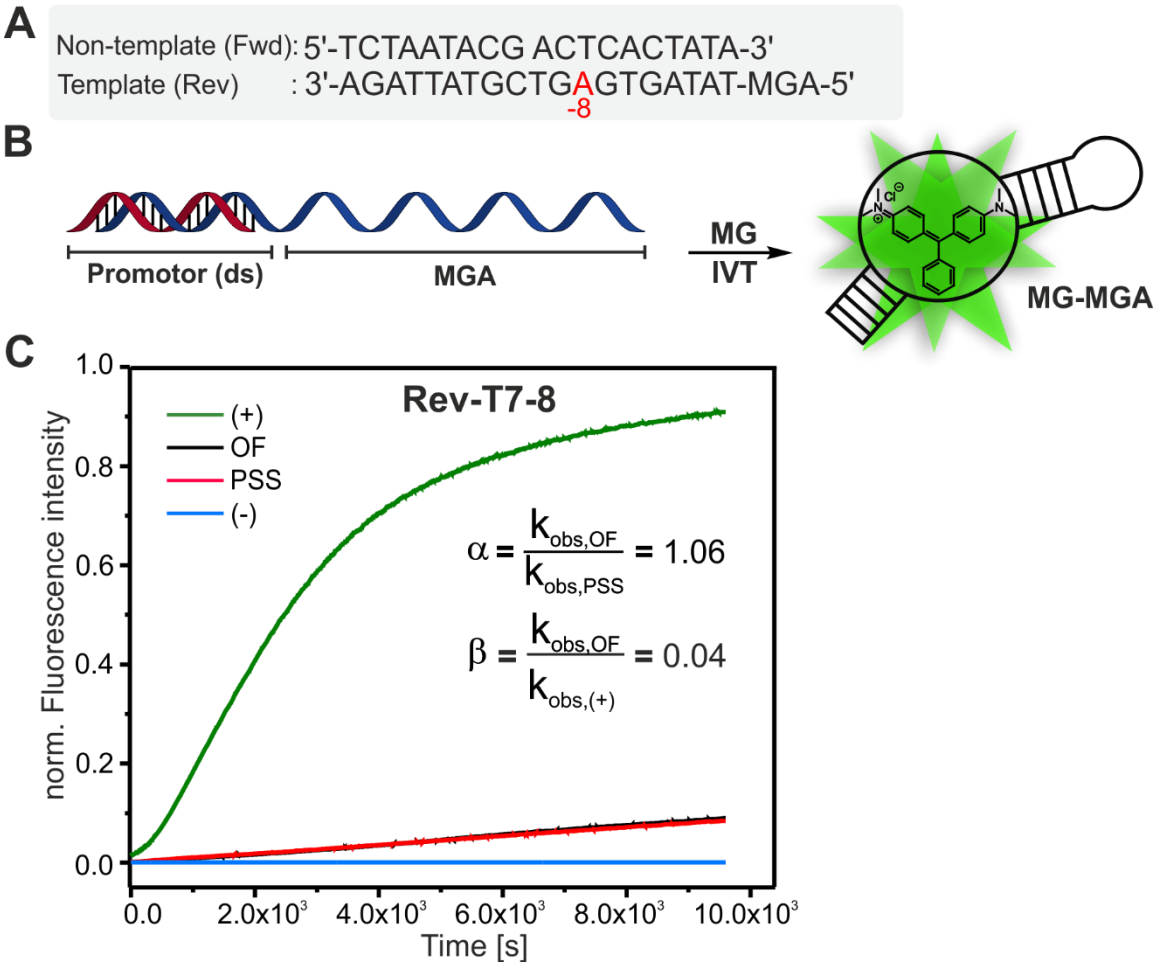

Figure S18: In vitro transcription of Rev-T7-8. (A) Sequence of the duplex promotor. The modified position is highlighted in red. (B) General design of the experiment. The photochromic nucleoside was incorporated into the templating strand of the T7 promotor linked to the sequence of the malachite green aptamer. Once the transcription is started, the aptamer is formed, which binds to its target malachite green, resulting in a fluorescent aptamer-dye complex. (C) Real time monitoring of the fluorescence during the in vitro transcription. The overall activity of the modified promotor is 4% compared to the positive control and a photoregulation efficiency of 1.06 was observed. The low α and β values indicate that a modification in the templating strand of the T7-Promotor sequence is not tolerated by the T7 RNA polymerase.

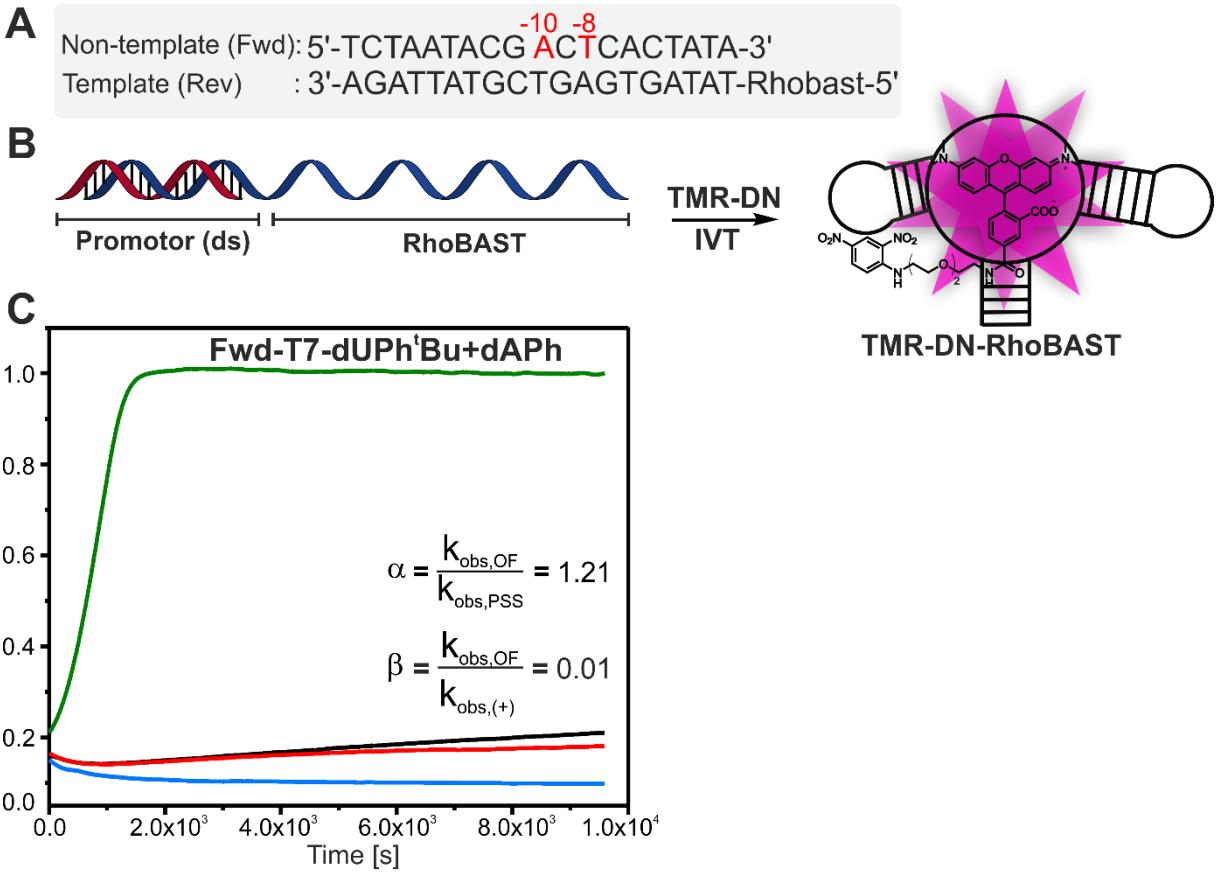

Figure S19: In vitro transcription of Rev-T7-8. (A) Sequence of the duplex promotor. The modified position is highlighted in red. (B) General design of the experiment. The photochromic nucleoside was incorporated into the templating strand of the T7 promotor linked to the sequence of the malachite green aptamer. Once the transcription is started, the aptamer is formed, which binds to its target malachite green, resulting in a fluorescent aptamer-dye complex. (C) Real time monitoring of the fluorescence during the in vitro transcription. The overall activity of the modified promotor is 1% compared to the positive control and a photoregulation efficiency of 1.21 was observed. The low α and β values indicate that two modifications in the non-templating strand of the T7 promotor sequence are not tolerated by the T7 RNA polymerase. We could not determine the melting temperature of the double modified promotor duplex, which suggests that the promotor is not double stranded during the transcription resulting in almost no activity of the T7-polymerase.

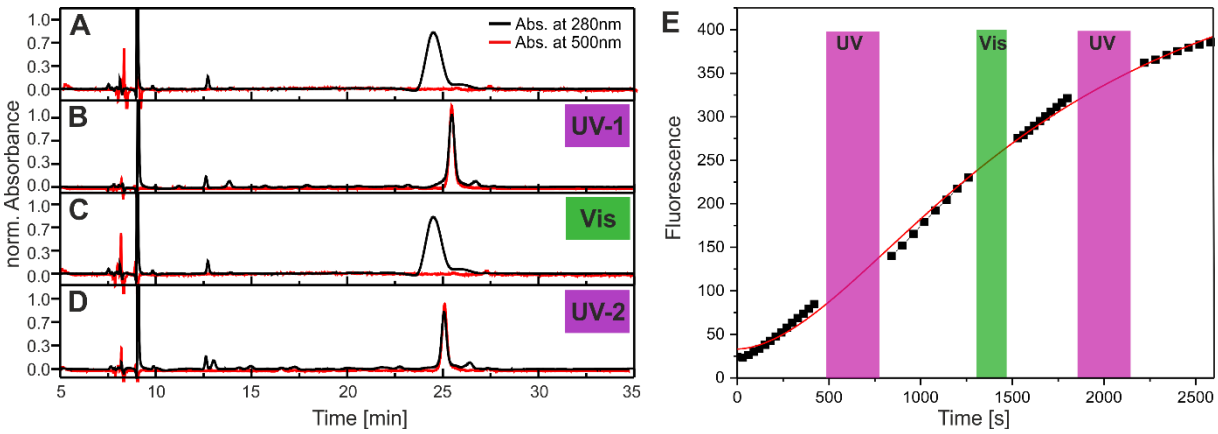

Figure S20 HPLC diagrams for monitoring the PSS^{UV} and photostability of Fwd-T7-10 (ds) during the irradiation conditions of the IVT switching experiment. Fwd-T7-10 (ss) was hybridized with its complementary strand in TRIS buffer (40 mM Tris-HCl, pH 7, 22 mM $MgCl_2$) by heating to 95°C for 5 min and subsequent snap cooling on ice. (A) Fwd-T7-10 (ds) before irradiation. (B) Fwd-T7-10 (ds) irradiated (UV1) with Xenon light source MAX-303 Asahi-Spectra (5 min, 320 nm, 3.5 W). A PSS^{UV} of 97% was reached without deterioration of the duplex. (C) Fwd-T7-10 (ds) irradiated (Vis) with Xenon light source MAX-303 Asahi-Spectra (3 min, 530 nm, 7.2 W). The open-ring isomer was completely recovered without deterioration of the duplex. (D) Fwd-T7-10 (ds) irradiated (UV2) with Xenon light source MAX-303 Asahi-Spectra (5 min, 320 nm, 3.5 W). Again a PSS^{UV} of 97% was generated without deterioration of the duplex. (E) IVT of the unmodified promotor sequence under the irradiation conditions of the IVT switching experiment. Irradiation of the IVT mixture containing the unmodified promotor sequence with UV and Vis light does not lead to any changes of the transcription rate. The progress of the IVT was fitted to a sigmoidal curve to emphasize that the irradiation cycles are harmless to all components of the mixture.

3-bromo-5-(4-methoxyphenyl)-2-methylthiophene (7^{PhOMe})

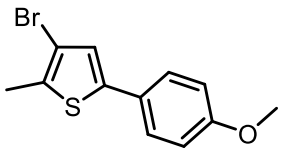

In a Schlenk flask under argon atmosphere, 4-bromo anisole (500 mg, 2.67 mmol, 1.00 eq.), 4-bromo-5-methylthiophene-2-ylboronic acid (680 mg, 3.07 mmol, 1.15 eq.), $Pd(PPh_3)_4$ (154 mg, 0.13 mmol, 0.05 eq.) and Na_2CO_3 (850 mg, 8.02 mmol, 3.00 eq.) were dissolved in a mixture of THF/Water (8/2 mL) and the mixture was stirred at 85°C overnight. Water and ethyl acetate were added and the organic phase was extracted with ethyl acetate for 3 times. The combined organic phases were washed with brine, dried over MgSO4 and filtered. The solvent was removed under reduced pressure and the crude product was purified by flash column chromatography (100/1, cyclohexane/ethyl acetate) which afforded 3-bromo-5-(4-methoxyphenyl)-2-methylthiophene (240 mg, 0.85 mmol, 32%) as a colourless solid.

^{1}H NMR (300 MHz, Chloroform-d) δ 7.43 (d, J = 8.9 Hz, 2H), 6.99 (s, 1H), 6.90 (d, J = 8.9 Hz, 2H), 3.83 (s, 3H), 2.40 (s, 3H).

^{13}C NMR (75 MHz, Chloroform-d) δ 159.54, 141.22, 132.70, 126.81, 126.53, 124.62, 114.48, 109.75, 77.16, 55.52, 14.92.

2-(4-bromo-5-methylthiophen-2-yl)pyrimidine (7^{Pym})

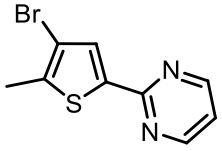

In a Schlenk flask under argon atmosphere, 2-bromopyrimidine (250 mg, 1.57 mmol, 1.00 eq.), 4-bromo-5-methylthiophene-2-ylboronic acid (452 mg, 2.04 mmol, 1.3 eq.), $Pd(PPh_3)_4$ (55 mg, 0.05 mmol, 0.05 eq.) and Na_2CO_3 (500 mg, 4.72 mmol, 3.00 eq.) were dissolved in THF/Water (8/2 mL) and the mixture was stirred at 85°C overnight. Water and ethyl acetate were added and the organic phase was extracted with ethyl acetate for 3 times. The combined organic phases were washed with brine, dried over $MgSO_4$ and filtered. The solvent was removed under reduced pressure and the crude product was purified by flash column chromatography (100/3, cyclohexane/ethyl acetate) which afforded 2-(4-bromo-5-methylthiophen-2-yl)pyrimidine (300 mg, 1.18 mmol, 75%) as a colourless solid.

^{1}H NMR (300 MHz, Chloroform-d) δ 8.67 (d, J = 4.9 Hz, 2H), 7.81 (s, 1H), 7.09 (t, J = 4.9 Hz, 1H), 2.46 (s, 3H).

^{13}C NMR (75 MHz, Chloroform-d) δ 160.67, 157.37, 139.54, 131.67, 118.79, 110.76, 77.16, 15.46.

2-(5-(4-methoxyphenyl)-2-methylthiophen-3-yl)-4,4,5,5-tetramethyl-1,3,2-dioxaborolane (8^{PhOMe})

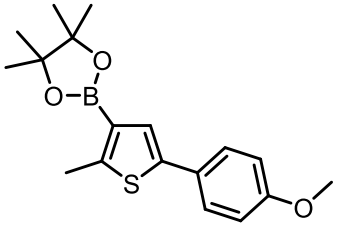

In a Schlenk flask under argon atmosphere, 3-bromo-5-(4-methoxyphenyl)-2-methylthiophene (230 mg, 0.81 mmol, 1.00 eq.), bis(pinacolato)diboron (248 mg, 0.97 mmol, 1.2 eq.), $Pd(PPh_3)_4$ (47 mg, 0.04 mmol, 0.05 eq.), XPhos (39 mg, 0.08 mmol, 0.10 eq.) and KOAc (239 mg, 2.44 mmol, 3.00 eq.) were dissolved in anhydrous dioxane (6 mL) and the mixture was stirred at 120°C overnight. Water and ethyl acetate were added and the organic phase was extracted with ethyl acetate for 3 times. The combined organic phases were washed with brine, dried over $MgSO_4$ and filtered. The solvent was removed under reduced pressure and the crude product was purified by flash column chromatography (100/2, cyclohexane/ethylacetate) which afforded 2-(5-(4-methoxyphenyl)-2-methylthiophen-3-yl)-4,4,5,5-tetramethyl-1,3,2-dioxaborolane (260 mg, 0.81 mmol, 97%) as a colourless oil.

^{1}H NMR (500 MHz, Chloroform-d) δ 7.49 (d, J = 8.8 Hz, 2H), 7.30 (s, 1H), 6.87 (d, J = 8.8 Hz, 2H), 3.82 (s, 3H), 2.69 (s, 3H), 1.33 (s, 12H).

^{13}C NMR (126 MHz, Chloroform-d) δ 158.89, 151.61, 140.91, 127.88, 127.57, 127.07, 114.27, 83.40, 77.16, 55.47, 25.06, 16.00.

2-(5-methyl-4-(4,4,5,5-tetramethyl-1,3,2-dioxaborolan-2-yl)thiophen-2-yl)pyrimidine (8^{Pym})

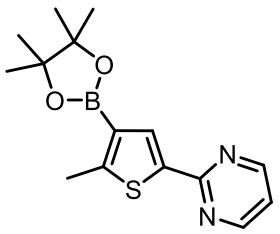

In a Schlenk flask under argon atmosphere, 2-(4-bromo-5-methylthiophen-2-yl)pyrimidine (300 mg, 1.18 mmol, 1.00 eq.), bis(pinacolato)diboron (388 mg, 1.53 mmol, 1.3 eq.), $Pd(PPh_3)_4$ (68 mg, 0.06 mmol, 0.05 eq.), XPhos (56 mg, 0.12 mmol, 0.10 eq.) and KOAc (346 mg, 3.46 mmol, 3.00 eq.) were dissolved in anhydrous dioxane (6 mL) and the mixture was stirred at 120°C overnight. Water and ethyl acetate were added and the organic phase was extracted with ethyl acetate for 3 times. The combined organic phases were washed with brine, dried over $MgSO_4$ and filtered. The solvent was removed under reduced pressure and the crude product was purified by flash column chromatography (100/4, cyclohexane/ethylacetate) which afforded 2-(5-methyl-4-(4,4,5,5-tetramethyl-1,3,2-dioxaborolan-2-yl)thiophen-2-yl)pyrimidine (205 mg, 0.68 mmol, 58%) as a colourless oil.

^{1}H NMR (300 MHz, Chloroform-d) δ 8.65 (d, J = 4.9 Hz, 2H), 8.15 (s, 1H), 7.03 (t, J = 4.9 Hz, 1H), 2.72 (s, 3H), 1.32 (s, 12H).

^{13}C NMR (75 MHz, Chloroform-d) δ 161.78, 157.41, 157.27, 139.67, 136.00, 118.08, 83.51, 77.16, 25.06, 16.43.

3-(2-bromocyclopent-1-en-1-yl)-5-(4-methoxyphenyl)-2-methylthiophene (9^{PhOMe})

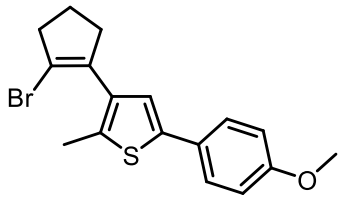

In a Schlenk flask under argon atmosphere, 2-(5-(4-methoxyphenyl)-2-methylthiophen-3-yl)-4,4,5,5-tetramethyl-1,3,2-dioxaborolane (200 mg, 0.61 mmol, 1.00 eq.), dibromocyclopentene (274 mg, 1.21 mmol, 2.0 eq.), $PdCl_2(PPh_3)_2$ (21 mg, 0.03 mmol, 0.05 eq.) and Cs_2CO_3 (493 mg, 1.51 mmol, 2.50 eq.) were dissolved in DMF (5 mL) and the mixture was stirred at 85°C overnight. Water and ethyl acetate were added and the organic phase was extracted with ethyl acetate for 3 times. The combined organic phases were washed with brine, dried over $MgSO_4$ and filtered. The solvent was removed under reduced pressure and the crude product was purified by flash column chromatography (100/1, cyclohexane/ethylacetate) which afforded 3-(2-bromocyclopent-1-en-1-yl)-5-(4-methoxyphenyl)-2-methylthiophene (130 mg, 0.38 mmol, 62%) as a yellow oil.

^{1}H NMR (500 MHz, Chloroform-d) δ 7.46 (d, J = 8.9 Hz, 2H), 7.00 (s, 1H), 6.89 (d, J = 8.9 Hz, 2H), 3.82 (s, 3H), 2.85 – 2.76 (m, 2H), 2.72 – 2.56 (m, 2H), 2.41 (s, 3H), 2.07 (p, J = 7.5 Hz, 2H).

^{13}C NMR (126 MHz, Chloroform-d) δ 159.06, 140.07, 136.76, 134.54, 134.42, 127.44, 126.87, 122.65, 118.78, 114.33, 77.16, 55.48, 41.10, 37.00, 22.62, 15.07.

2-(4-(2-bromocyclopent-1-en-1-yl)-5-methylthiophen-2-yl)pyrimidine (9^{Pym})

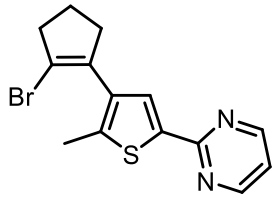

In a Schlenk flask under argon atmosphere, 2-(5-methyl-4-(4,4,5,5-tetramethyl-1,3,2-dioxaborolan-2-yl)thiophen-2-yl)pyrimidine (200 mg, 0.61 mmol, 1.00 eq.), dibromocyclopentene (274 mg, 1.21 mmol, 2.0 eq.), $PdCl_2(PPh_3)_2$ (21 mg, 0.03 mmol, 0.05 eq.) and Cs_2CO_3 (493 mg, 1.51 mmol, 2.50 eq.) were dissolved in DMF (5 mL) and the mixture was stirred at 85°C overnight. Water and ethyl acetate were added and the organic phase was extracted with ethyl acetate for 3 times. The combined organic phases were washed with brine, dried over $MgSO_4$ and filtered. The solvent was removed under reduced pressure and the crude product was purified by flash column chromatography (100/1, cyclohexane/ethylacetate) which afforded 3-(2-bromocyclopent-1-en-1-yl)-5-(4-methoxyphenyl)-2-methylthiophene (130 mg, 0.38 mmol, 62%) as a yellow oil.

^{1}H NMR (300 MHz, Chloroform-d) δ 8.67 (d, J = 5.3 Hz, 2H), 7.81 (s, 1H), 7.05 (d, J = 4.9 Hz, 1H), 2.82 (ddt, J = 8.1, 4.9, 2.4 Hz, 2H), 2.66 (tt, J = 7.8, 2.4 Hz, 2H), 2.46 (s, 3H), 2.08 (p, J = 7.3 Hz, 2H).

^{13}C NMR (75 MHz, Chloroform-d) δ 157.29, 141.28, 136.80, 136.37, 135.29, 128.58, 119.44, 118.23, 77.16, 41.12, 37.01, 22.65, 15.50.

2-(2-(5-(4-methoxyphenyl)-2-methylthiophen-3-yl)cyclopent-1-en-1-yl)-4,4,5,5-tetramethyl-1,3,2-dioxaborolane (10^{PhOMe})

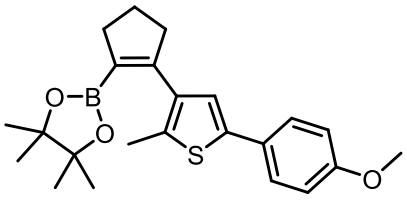

In a Schlenk flask under argon atmosphere, 3-(2-bromocyclopent-1-en-1-yl)-5-(4-methoxyphenyl)-2-methylthiophene (130 mg, 0.30 mmol, 1.00 eq.), bis(pinacolato)diboron (357 mg, 0.91 mmol, 1.2 eq.), $Pd(PPh_3)_4$ (17 mg, 0.01 mmol, 0.05 eq.), XPhos (14 mg,

0.03 mmol, 0.10 eq.) and KOAc (73 mg, 0.74 mmol, 2.50 eq.) were dissolved in anhydrous dioxane (6 mL) and the mixture was stirred at 120°C overnight. Water and ethyl acetate were added and the organic phase was extracted with ethyl acetate for 3 times. The combined organic phases were washed with brine, dried over $MgSO_4$ and filtered. The solvent was removed under reduced pressure and the crude product was purified by flash column chromatography (100/2, cyclohexane/ethylacetate) which afforded 2-(2-(5-(4-methoxyphenyl)-2-methylthiophen-3-yl)cyclopent-1-en-1-yl)-4,4,5,5-tetramethyl-1,3,2-dioxaborolane (57 mg, 0.14 mmol, 48%) as a yellow oil.

^{1}H NMR (300 MHz, Chloroform-d) δ 7.46 (d, J = 8.9 Hz, 2H), 7.02 (s, 1H), 6.88 (d, J = 8.9 Hz, 2H), 3.82 (s, 3H), 2.77 – 2.58 (m, 4H), 2.37 (s, 3H), 1.93 (p, J = 7.7 Hz, 2H), 1.19 (s, 12H).

^{13}C NMR (75 MHz, Chloroform-d) δ 159.01, 158.79, 152.28, 138.50, 137.59, 133.49, 127.84, 126.59, 124.27, 114.28, 83.02, 77.16, 55.48, 40.40, 37.29, 24.97, 24.47, 14.70.

2-(5-methyl-4-(2-(4,4,5,5-tetramethyl-1,3,2-dioxaborolan-2-yl)cyclopent-1-en-1-yl)thiophen-2-yl)pyrimidine (10^{Pym})

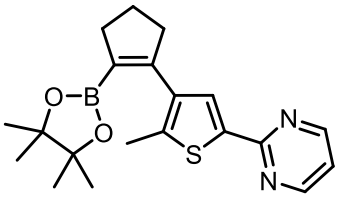

In a Schlenk flask under argon atmosphere, 2-(4-(2-bromocyclopent-1-en-1-yl)-5-methylthiophen-2-yl)pyrimidine (130 mg, 0.30 mmol, 1.00 eq.), bis(pinacolato)diboron (357 mg, 0.91 mmol, 1.2 eq.), $Pd(PPh_3)_4$ (17 mg, 0.01 mmol, 0.05 eq.), XPhos (14 mg, 0.03 mmol, 0.10 eq.) and KOAc (73 mg, 0.74 mmol, 2.50 eq.) were dissolved in anhydrous dioxane (6 mL) and the mixture was stirred at 120°C overnight. Water and ethyl acetate were added and the organic phase was extracted with ethyl acetate for 3 times. The combined organic phases were washed with brine, dried over $MgSO_4$ and filtered. The solvent was removed under reduced pressure and the crude product was purified by flash column chromatography (100/2, cyclohexane/ethylacetate) which afforded 2-(2-(5-(4-methoxyphenyl)-2-methylthiophen-3-yl)cyclopent-1-en-1-yl)-4,4,5,5-tetramethyl-1,3,2-dioxaborolane (57 mg, 0.14 mmol, 48%) as a yellow oil.

^{1}H NMR (300 MHz, Chloroform-d) δ 8.64 (d, J = 4.9 Hz, 2H), 7.79 (s, 1H), 7.02 (t, J = 4.9 Hz, 1H), 2.67 (ddt, J = 13.9, 9.5, 4.8 Hz, 4H), 2.42 (s, 3H), 1.93 (p, J = 7.5 Hz, 2H), 1.18 (s, 12H).

^{13}C NMR (75 MHz, cdcl3) δ 161.89, 157.23, 152.01, 140.50, 138.49, 137.47, 131.33, 117.93, 83.03, 77.16, 40.50, 37.26, 24.96, 24.42, 15.10.

4-chloro-7-(phenylsulfonyl)-7H-pyrrolo[2,3-d]pyrimidine (12)

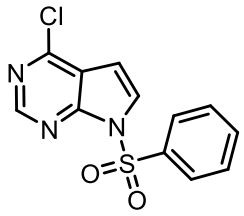

In a flame-dried schlenk flask und argon atmosphere, 4-chloro-7,7a-dihydro-6H-pyrrolo[2,3-d]pyrimidine (16.0 g, 103 mmol, 1.0 eq) was dissolved in anhydrous THF (500 mL) and the mixture was cooled to 0 °C. Then, sodium hydride (6.4 g, 276 mmol, 2.5 eq) was added portion wise and the mixture was stirred for 3 h at 0 °C. Afterwards, benzenesulfonyl chloride (27.5 g, 156 mmol, 1.5 eq) was added and the mixture was allowed to warm up to RT and stirred overnight. Then, a saturated ammonium chloride solution was added and the mixture was extracted with ethyl acetate for 3 times. The combined organic phases were dried over anhydrous Mg_2SO_4 and the amount of solvent was reduced until a colourless precepitate appeared. Filtration afforded 4-chloro-7-(phenylsulfonyl)-7H-pyrrolo[2,3-d]pyrimidine (24.8 g, 84.5 mmol, 82%) as a colourless solid.

^{1}H NMR (300 MHz, DMSO-d_6) δ 8.82 (s, 1H), 8.22 – 8.08 (m, 3H), 7.85 – 7.73 (m, 1H), 7.72 – 7.61 (m, 2H), 6.97 (d, *J* = 4.1 Hz, 1H).

4-chloro-6-methyl-7H-pyrrolo[2,3-d]pyrimidine (13)

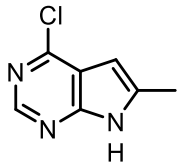

In a flame-dried schlenk flask under argon atmosphere, 4-chloro-7-(phenylsulfonyl)-7H-pyrrolo[2,3-d]pyrimidine (12 g, 40.8 mmol, 1.00 eq) was dissolved in anhydrous THF (250 mL) and cooled to -78 °C. Then *n*-buthyl lithium (2.5 M in hexane, 26.2 mL, 65.4 mmol, 1.60 eq) and TEMEDA (12.3 mL, 81.7 mmol, 2.00 eq) were added simultaneously (*n*-buthyl lithium always in excess) over a period of 30 min and stirred for additional 30 min. Afterwards, iodomethane (12.7 mL, 204 mmol, 5.00 eq) was added and the mixture was allowed to warm to RT and stirred overnight. Then, a saturated ammonium chloride solution was added and the mixture was extracted with ethyl acetate for 3 times. The combined organic phases were dried over anhydrous Mg_2SO_4 and the solvent was removed under reduced pressure. The brown residue was dissolved in dry THF and transferred to a flame-dried Schlenk flask under argon

atmosphere. The reaction mixture was treated portion-wise with potassium tertbutoxide (22.9 g, 204 mmol, 5 eq) at 0 °C and stirred at RT overnight. Then, a saturated sodium chloride solution was added and the mixture was extracted with ethyl acetate for 3 times. The combined organic phases were washed with water for 3 times and dried over anhydrous Mg_2SO_4. The solvent was removed under reduced pressure and the crude product was purified via flash column chromatography (cyclohexane/ ethyl acetate (2/1)), which yielded 4-chloro-6-methyl-7H-pyrrolo[2,3-d]pyrimidine (4.6 g, 27.4 mmol, 67 as a brown solid.

^{1}H NMR (300 MHz, DMSO-d_6) δ 8.48 (s, 1H), 6.30 (s, 1H), 2.43 (s, 3H).

4-chloro-5-iodo-6-methyl-7H-pyrrolo[2,3-d]pyrimidine (14)

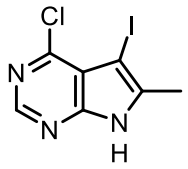

In a 100 mL flask, 4-chloro-6-methyl-7H-pyrrolo[2,3-d]pyrimidine (1.1 g, 6.60 mmol, 1.00 eq) was suspended in DCM (50 mL). Then, NIS (1.7 g, 7.70 mmol, 1.16 eq) was added portion wise and the reaction mixture was stirred RT for 1.5 h. The precipitate was filtered was filtered of and washed with cold DCM. 4-chloro-5-iodo-6-methyl-7H-pyrrolo[2,3-d]pyrimidine (1.20 g, 4.10 mmol, 63%) could be obtained as colourless solid.

^{1}H NMR (300 MHz, DMSO-d_6) δ 12.93 (s, 1H), 8.51 (s, 1H), 2.42 (s, 3H).

(2S,3S)-5-(4-chloro-5-iodo-6-methyl-7H-pyrrolo[2,3-d]pyrimidin-7-yl)-2-(((4-methyl-benzoyl)oxy)-methyl)tetrahydrofuran-3-yl 4-methylbenzoate (15)

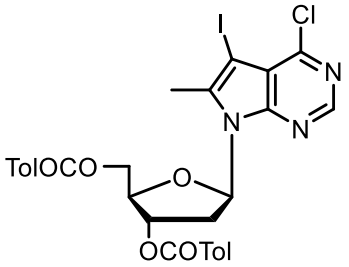

In a flame dried schlenk flask under argon atmosphere, 4-chloro-5-iodo-6-methyl-7H-pyrrolo[2,3-d]pyrimidine (1.20 g, 4.10 mmol, 1.00 eq) was suspended in anhydrous acetonitrile (35 mL). Powdered potassium hydroxide (920 mg, 16.4 mmol, 4.00 eq) was added and the mixture was stirred for 1 h at RT. Afterwards, TDA-1 (223 mg, 0.69 mmol, 0.17 eq) and hoffer's chlorosugar (2.00 g, 5.33 mmol, 1.30 eq) were added and the mixture was stirred for another 1.5 h. The formed precipitate was filtered and the filtrate was concentrated under reduced pressure. The crude product was purified via flash column chromatography (cyclohexane/ ethyl acetate (4/1), which yielded (2S,3S)-5-(4-chloro-5-iodo-6-methyl-7H-pyrrolo[2,3-d]pyrimidin-7-

yl)-2-(((4-methylbenzoyl)oxy)-methyl)tetrahydrofuran-3-yl4-methyl-benzoate (1.30 g, 2.05 mmol, 50%) as a yellow oil.

^{1}H NMR (300 MHz, Chloroform-*d*) δ 8.48 (s, 1H), 7.97 (d, *J* = 8.2 Hz, 2H), 7.86 (d, *J* = 8.2 Hz, 2H), 7.29 (d, *J* = 8.0 Hz, 2H), 7.20 (d, *J* = 8.0 Hz, 2H), 6.56 (t, *J* = 7.1 Hz, 1H), 5.95 (dt, *J* = 7.7, 3.6 Hz, 1H), 4.80 (dd, *J* = 11.8, 4.0 Hz, 1H), 4.66 – 4.48 (m, 2H), 3.75 (dt, *J* = 14.3, 7.4 Hz, 1H), 2.63 (s, 3H), 2.60 – 2.52 (m, 1H), 2.44 (s, 3H), 2.41 (s, 3H).

^{13}C NMR (75 MHz, $cdcl_3$) δ 166.33, 166.17, 151.96, 151.48, 149.83, 144.56, 144.10, 141.40, 129.94, 129.82, 129.42, 129.25, 126.95, 126.73, 117.72, 85.03, 82.08, 77.16, 74.68, 63.67, 56.96, 36.12, 21.86, 15.25.

MS (HR-ESI, positive) m/z: $[M+Na]^+$ calculated for $C_{28}H_{25}ClIN_3O_5Na^+$: 668.0420, found: 668.0428.

(2S,3S)-5-(4-amino-5-iodo-6-methyl-7H-pyrrolo[2,3-d]pyrimidin-7-yl)-2-(hydroxymethyl)tetrahydrofuran-3-ol (1)

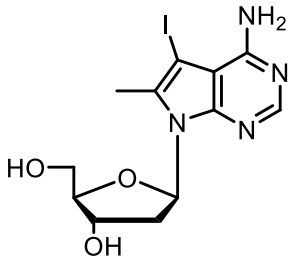

In a microwave vial, (2S,3S)-5-(4-chloro-5-iodo-6-methyl-7H-pyrrolo[2,3-d]pyrimidin-7-yl)-2-(((4-methylbenzoyl)oxy)-methyl)tetrahydrofuran-3-yl4-methyl-benzoate (400 mg, 0.62 mmol, 1.00 eq) was dissolved in a mixture of dioxane (1.5 mL) and aqueous NH_3 (3 mL, 25%). The mixture stirred for 6 h at 150 °C in a microwave reactor (150 W, 20 bar, power max: on, stirring: on). Afterwards the solvent was removed under reduced pressure and the crude product was purified via reverse phase column chromatography (water/acetonitrile + 0.1% TFA), which yielded (2S,3S)-5-(4-amino-5-iodo-6-methyl-7H-pyrrolo[2,3-d]pyrimidin-7-yl)-2-(hydroxylmethyl)tetrahydrofuran-3-ol (242 mg, 0.62 mmol, quant.) as a pale yellow solid.

^{1}H NMR (300 MHz, DMSO-d_6) δ 8.25 (s, 1H), 7.30 – 6.90 (m, 1H), 6.49 (t, *J* = 7.5 Hz, 1H), 4.44 – 4.35 (m, 1H), 3.80 (q, *J* = 4.1 Hz, 1H), 3.68 – 3.47 (m, 2H), 2.91 – 2.74 (m, 1H), 2.47 (s, 3H), 2.20 – 2.05 (m, 1H).

MS (HR-ESI, positive) m/z: $[M+H]^+$ calculated for $C_{12}H_{16}IN_4O_3^+$: 391.0262, found: 391.0283.

General procedure A for the synthesis of photoswitchable 2'-deoxy-7-deaza-adenosine nucleosides (2^R)

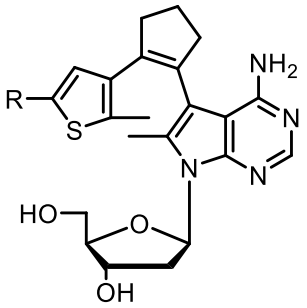

In a microwave vial under argon atmosphere, **11** (0.1 mmol), $\mathbf{5^R}$ (0.13 mmol), $Pd(PPh_3)_4$ (5 µmol) and Na_2CO_3 (0.3 mmol) were dissolved in DME/water (2/1) and stirred at 80°C until the starting material **11** was consumed completely (monitored via TLC). Water and ethyl acetate were added to the mixture and the aqueous phase was extracted with ethyl acetate 3 times. The combined organic phases were washed with brine, dried over anhydrous $MgSO_4$ and the solvent was removed under reduced pressure. The crude product was purified via reverse phase column chromatography (water/acetonitrile + 0.1% TFA) affording $\mathbf{12^R}$.

5-(4-amino-5-(2-(5-(4-methoxyphenyl)-2-methylthiophen-3-yl)cyclopent-1-en-1-yl)-6-methyl-7H-pyrrolo[2,3-d]pyrimidin-7-yl)-2-(hydroxymethyl)tetrahydrofuran-3-ol (2^{PhOMe})

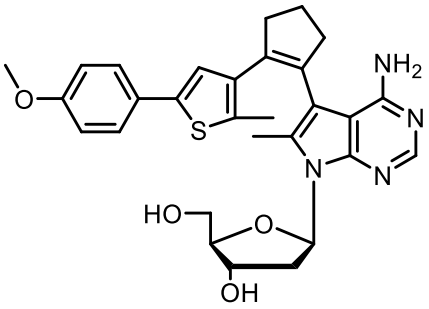

The photoswitchable 2'-deoxy-7-deaza-adenosine nucleoside $\mathbf{dA^{PhOMe}}$ was prepared according to the general procedure A. Purification via reverse phase column chromatography afforded $\mathbf{dA^{PhOMe}}$ as a colourless solid with a yield of 56%.

^{1}H NMR (500 MHz, DMSO-d6) δ 8.31 (s, 1H), 7.96 (d, J = 1.7 Hz, 1H), 7.32 (dd, J = 11.0, 8.8 Hz, 2H), 6.99 (d, J = 13.0 Hz, 1H), 6.90 (dd, J = 8.8, 1.6 Hz, 2H), 6.34 – 6.26 (m, 1H), 5.63 (dd, J = 7.9, 3.5 Hz, 0H), 5.52 (dd, J = 7.6, 3.7 Hz, 0H), 5.21 (s, 1H), 4.43 – 4.31 (m, 1H), 3.85 – 3.78 (m, 1H), 3.74 (s, 3H), 3.67 – 3.58 (m, 1H), 3.50 (q, J = 9.6, 7.6 Hz, 1H), 3.03 – 2.71 (m, 4H), 2.68 – 2.56 (m, 1H), 2.10 (d, J = 15.8 Hz, 3H), 2.06 – 2.00 (m, 2H), 1.98 (s, 3H).

^{13}C NMR (126 MHz, DMSO-d6) δ 158.55, 156.61, 156.58, 150.25, 150.23, 149.65, 149.59, 138.20, 138.11, 137.59, 137.34, 135.84, 135.74, 132.51, 132.39, 132.21, 132.13, 129.36, 129.11, 126.42, 126.39, 126.10, 126.03, 123.20, 123.18, 109.18, 109.14, 101.56, 101.44,

87.40, 83.93, 83.78, 71.24, 71.15, 62.25, 62.12, 55.17, 39.52, 37.69, 22.65, 22.63, 14.19, 14.16, 11.08, 10.96.

MS (HR-ESI, positive) m/z: $[M+H]^+$ calculated for $C_{29}H_{33}N_4O_4S^+$: 553.2217, found: 553.2197.

5-(4-amino-6-methyl-5-(2-(2-methyl-5-(naphthalen-2-yl)thiophen-3-yl)cyclopent-1-en-1-yl)-7H-pyrrolo[2,3-d]pyrimidin-7-yl)-2-(hydroxymethyl)tetrahydrofuran-3-ol (2^{Np})

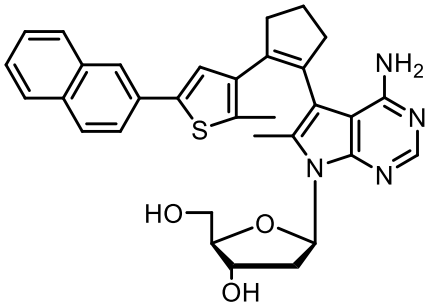

The photoswitchable 2'-deoxy-7-deaza-adenosine nucleoside **dA^{Np}** was prepared according to the general procedure A. Purification via reverse phase column chromatography afforded **dA^{Np}** as a colourless solid with a yield of 70%.

^{1}H NMR (500 MHz, Methanol-d4) δ 8.12 (s, 1H), 7.81 (dd, 4H), 7.59 – 7.51 (m, 1H), 7.44 (dt, J = 16.0, 7.2 Hz, 2H), 7.15 (d, J = 15.3 Hz, 1H), 6.46 (t, J = 14.7 Hz, 1H), 4.63 – 4.50 (m, 1H), 4.00 (p, J = 3.8 Hz, 1H), 3.78 (ddt, J = 48.3, 12.0, 3.6 Hz, 2H), 3.14 – 2.90 (m, 3H), 2.89 – 2.76 (m, 2H), 2.33 (d, J = 14.3 Hz, 3H), 2.29 – 2.16 (m, 3H), 2.09 (s, 3H).

^{13}C NMR (75 MHz, DMSO-d6) δ 158.47, 151.50, 147.67, 138.99, 138.75, 138.49, 138.39, 135.85, 135.72, 134.46, 134.32, 133.21, 132.69, 132.27, 132.06, 131.55, 131.42, 131.05, 130.58, 130.50, 128.59, 127.77, 127.59, 126.74, 125.99, 124.90, 123.43, 122.72, 111.36, 100.26, 87.21, 83.33, 70.46, 61.50, 45.69, 39.52, 37.85, 22.49, 14.28, 11.39.

MS (HR-ESI, positive) m/z: $[M+H]^+$ calculated for $C_{32}H_{33}N_4O_3S^+$: 553.2268, found: 553.2274.

5-(4-amino-6-methyl-5-(2-(2-methyl-5-phenylthiophen-3-yl)cyclopent-1-en-1-yl)-7H-pyrrolo[2,3-d]pyrimidin-7-yl)-2-(hydroxymethyl)tetrahydrofuran-3-ol (2^{Ph})

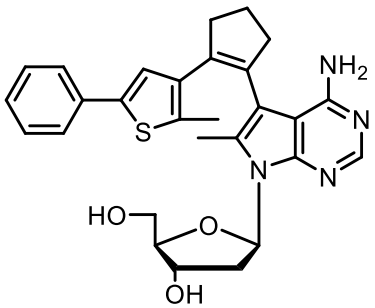

The photoswitchable 2'-deoxy-7-deaza-adenosine nucleoside **dA^{Ph}** was prepared according to the general procedure A. Purification via reverse phase column chromatography afforded **dA^{Ph}** as a colourless solid with a yield of 62%.

^{1}H NMR (500 MHz, DMSO-d6) δ 7.96 (d, J = 2.0 Hz, 1H), 7.40 (dd, J = 12.7, 7.8 Hz, 2H), 7.34 (t, J = 6.8 Hz, 2H), 7.23 (t, J = 7.1 Hz, 1H), 7.14 (d, J = 16.3 Hz, 1H), 6.35 – 6.25 (m, 1H), 5.57 (d, 1H), 5.23 (s, 1H), 4.37 (dd, J = 20.1, 4.5 Hz, 1H), 3.86 – 3.75 (m, 1H), 3.68 – 3.58 (m, 1H), 3.55 – 3.45 (m, 1H), 3.04 – 2.71 (m, 4H), 2.64 (dt, J = 15.9, 8.2 Hz, 2H), 2.10 (d, J = 16.4 Hz, 3H), 2.07 – 2.02 (m, 1H), 2.01 (d, J = 4.4 Hz, 3H).

^{13}C NMR (75 MHz, dmso) δ 156.57, 150.26, 149.67, 149.61, 138.18, 138.07, 137.48, 137.23, 136.03, 135.92, 133.76, 133.64, 132.41, 132.32, 129.38, 129.12, 128.99, 127.15, 124.74, 124.67, 124.43, 109.15, 101.40, 87.39, 83.93, 83.77, 71.13, 62.23, 62.10, 39.52, 37.66, 22.64, 14.24, 11.08.

MS (HR-ESI, positive) m/z: $[M+H]^+$ calculated for $C_{28}H_{31}N_4O_3S^+$: 489.1955, found: 489.1961.

5-(4-amino-5-(2-(5-(3,5-bis(trifluoromethyl)phenyl)-2-methylthiophen-3-yl)cyclopent-1-en-1-yl)-6-methyl-7H-pyrrolo[2,3-d]pyrimidin-7-yl)-2-(hydroxymethyl)tetrahydrofuran-3-ol (2$^{Ph(CF_3)_2}$)

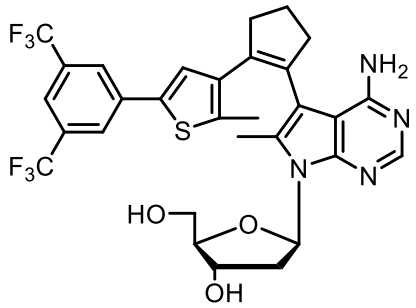

The photoswitchable 2'-deoxy-7-deaza-adenosine nucleoside **dA$^{Ph(CF_3)_2}$** was prepared according to the general procedure A. Purification via reverse phase column chromatography afforded **dA$^{Ph(CF_3)_2}$** as a colourless solid with a yield of 71%.

^{1}H NMR (300 MHz, DMSO-d6) δ 8.29 (d, J = 2.9 Hz, 1H), 8.04 (d, J = 10.3 Hz, 2H), 7.95 (s, 1H), 7.66 (d, J = 18.6 Hz, 1H), 6.52 – 6.33 (m, 1H), 4.45 – 4.25 (m, 1H), 3.83 – 3.69 (m, 1H), 3.65 – 3.41 (m, 2H), 3.04 – 2.79 (m, 3H), 2.78 – 2.55 (m, 2H), 2.16 (d, J = 14.4 Hz, 3H), 2.12 – 2.01 (m, 2H), 1.95 (d, J = 2.1 Hz, 3H).

^{13}C NMR (75 MHz, DMSO-d6) δ 161.15, 159.02, 158.58, 151.15, 147.47, 138.61, 138.35, 136.65, 136.48, 136.43, 136.30, 136.11, 134.95, 134.85, 132.92, 132.47, 131.35, 130.97, 130.91, 130.88, 130.48, 124.94, 121.32, 111.47, 111.27, 100.13, 99.98, 87.17, 70.35, 61.62,

61.38, 40.36, 40.08, 39.80, 39.52, 39.34, 39.24, 38.96, 38.69, 38.38, 37.99, 22.42, 14.20, 11.40.

^{19}F NMR (282 MHz, DMSO-d6) δ -61.54.

MS (HR-ESI, positive) m/z: $[M+H]^+$ calculated for $C_{30}H_{29}F_6N_4O_3S^+$: 639.1859, found: 639.1855.

5-(4-amino-6-methyl-5-(2-(2-methyl-5-(pyridin-2-yl)thiophen-3-yl)cyclopent-1-en-1-yl)-7H-pyrrolo[2,3-d]pyrimidin-7-yl)-2-(hydroxymethyl)tetrahydrofuran-3-ol (2^{2Py})

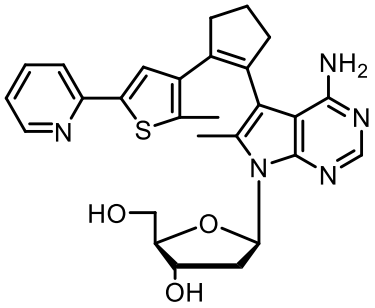

The photoswitchable 2'-deoxy-7-deaza-adenosine nucleoside **dA^{2Py}** was prepared according to the general procedure A. Purification via reverse phase column chromatography afforded **dA^{2Py}** as a colourless solid with a yield of 65%.

^{1}H NMR (300 MHz, DMSO-d_6) δ 8.45 (dt, *J* = 4.8, 1.4 Hz, 1H), 8.31 (d, *J* = 5.1 Hz, 1H), 7.77 (tt, *J* = 7.6, 1.6 Hz, 1H), 7.72 – 7.59 (m, 1H), 7.46 (t, *J* = 9.0 Hz, 1H), 7.21 (ddd, *J* = 7.5, 4.9, 1.1 Hz, 1H), 6.45 (dt, *J* = 19.2, 7.3 Hz, 1H), 4.35 (ddd, *J* = 14.5, 6.9, 3.5 Hz, 1H), 3.77 (p, *J* = 4.1 Hz, 1H), 3.69 – 3.39 (m, 2H), 2.83 (dq, *J* = 15.3, 7.5 Hz, 5H), 2.28 – 2.03 (m, 6H), 1.98 (d, *J* = 1.2 Hz, 3H).

^{13}C NMR (75 MHz, DMSO-d_6) δ 159.12, 158.34, 151.95, 149.66, 140.16, 140.11, 139.69, 139.45, 137.53, 137.41, 137.29, 136.05, 135.94 133.34, 130.38, 130.29, 127.55, 121.64, 118.96, 112.60, 112.41, 112.22, 101.05, 87.51, 83.65, 71.51, 70.33, 62.37, 61.24, 54.47, 22.82, 15.62, 11.13.

5-(4-amino-6-methyl-5-(2-(2-methyl-5-(pyrimidin-2-yl)thiophen-3-yl)cyclopent-1-en-1-yl)-7H-pyrrolo[2,3-d]pyrimidin-7-yl)-2-(hydroxymethyl)tetrahydrofuran-3-ol (2^{Pym})

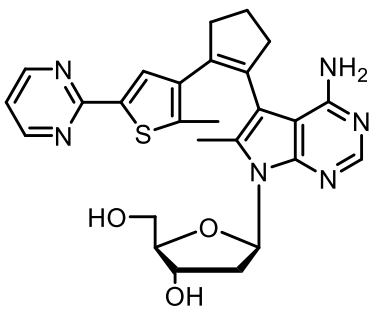

The photoswitchable 2'-deoxy-7-deaza-adenosine nucleoside **dA^{Pym}** was prepared according to the general procedure A. Purification via reverse phase column chromatography afforded **dA^{Pym}** as a colourless solid with a yield of 48%.

^{1}H NMR (300 MHz, DMSO-d6) δ 8.71 (d, J = 4.9 Hz, 2H), 8.19 (d, J = 2.6 Hz, 1H), 7.67 (d, J = 4.5 Hz, 1H), 7.28 (t, J = 4.7 Hz, 1H), 6.47 – 6.28 (m, 1H), 4.42 – 4.27 (m, 1H), 3.82 – 3.72 (m, 1H), 3.60 – 3.47 (m, 3H), 2.90 (s, 2H), 2.81 – 2.71 (m, 1H), 2.71 – 2.58 (m, 1H), 2.15 (d, J = 10.7 Hz, 3H), 2.12 – 2.04 (m, 2H), 2.02 (d, J = 4.5 Hz, 3H).

^{13}C NMR (75 MHz, DMSO-d6) δ 160.10, 158.33, 157.90, 157.56, 139.30, 138.42, 138.04, 131.10, 129.68, 118.95, 110.83, 100.54, 87.32, 83.73, 83.34, 70.71, 70.48, 61.77, 61.49, 57.91, 45.71, 39.52, 37.87, 22.45, 14.53, 11.32, 8.61, 7.61.

MS (HR-ESI, positive) m/z: $[M+H]^+$ calculated for $C_{26}H_{28}F_6N_6O_3SNa^+$: 527.1836, found: 527.1841.

4-(4-(2-(4-amino-7-((2R,4S,5R)-4-hydroxy-5-(hydroxymethyl)tetrahydrofuran-2-yl)-6-methyl-7H-pyrrolo[2,3-d]pyrimidin-5-yl)cyclopent-1-en-1-yl)-5-methylthiophen-2-yl)benzoate (2$^{Ph^tBu}$)

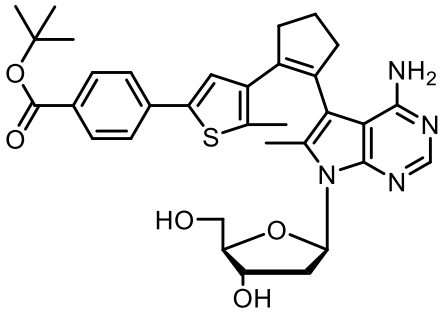

The photoswitchable 2'-deoxy-7-deaza-adenosine nucleoside **dA$^{Pht^{Bu}}$** was prepared according to the general procedure A. Purification via reverse phase column chromatography afforded **dA$^{Pht^{Bu}}$** as a colourless solid with a yield of 58%.

^{1}H NMR (300 MHz, DMSO-d6) δ 8.31 (d, J = 4.5 Hz, 1H), 7.86 (dd, J = 8.5, 1.2 Hz, 2H), 7.54 (dd, J = 8.5, 2.6 Hz, 2H), 7.30 (d, J = 7.4 Hz, 1H), 6.45 (dt, J = 14.8, 7.4 Hz, 1H), 4.37 (ddd, J = 15.6, 6.9, 3.5 Hz, 1H), 3.85 – 3.72 (m, 1H), 3.67 – 3.43 (m, 2H), 3.07 – 2.83 (m, 2H), 2.79 – 2.58 (m, 2H), 2.20 (d, J = 17.5 Hz, 3H), 2.16 – 2.05 (m, 2H), 2.02 (s, 3H), 1.54 (s, 9H).

^{13}C NMR (75 MHz, DMSO-d6) δ 164.51, 150.32, 147.20, 139.07, 138.85, 137.53, 137.18, 136.04, 135.94, 135.78, 133.38, 133.11, 132.98, 130.46, 130.34, 129.84, 129.58, 128.98, 128.72, 125.98, 124.57, 111.80, 111.64, 99.96, 87.28, 83.55, 83.25, 80.71, 61.56, 61.37, 39.52, 27.80, 22.42, 14.20, 11.39, 11.25.

MS (HR-ESI, positive) m/z: $[M+H]^+$ calculated for $C_{33}H_{38}N_4O_5SNa^+$: 625.2455, found: 625.2466.

5-(4-amino-6-methyl-5-(2-(2-methyl-5-(4-nitrophenyl)thiophen-3-yl)cyclopent-1-en-1-yl)-7H-pyrrolo[2,3-d]pyrimidin-7-yl)-2-(hydroxymethyl)tetrahydrofuran-3-ol (2^{PhNO_2})

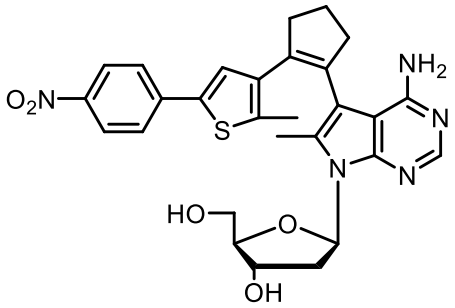

The photoswitchable 2'-deoxy-7-deaza-adenosine nucleoside **dA^{PhNO_2}** was prepared according to the general procedure A. Purification via reverse phase column chromatography afforded **dA^{PhNO_2}** as a colourless solid with a yield of 38%.

^{1}H NMR (300 MHz, DMSO-d6) δ 8.19 (dd, J = 8.9, 1.6 Hz, 2H), 7.96 (d, J = 2.3 Hz, 1H), 7.69 (dd, J = 8.9, 6.0 Hz, 2H), 7.48 (d, J = 10.1 Hz, 1H), 6.34 – 6.24 (m, 2H), 5.20 (d, J = 3.6 Hz, 1H), 4.44 – 4.27 (m, 1H), 3.80 (q, J = 3.5, 2.9 Hz, 1H), 3.68 – 3.55 (m, 1H), 3.55 – 3.42 (m, 1H), 2.91 – 2.72 (m, 3H), 2.71 – 2.56 (m, 1H), 2.09 (d, J = 12.6 Hz, 3H), 2.06 – 2.02 (m, 1H), 2.02 – 1.99 (m, 3H).

^{13}C NMR (75 MHz, DMSO-d6) δ 156.37, 150.06, 149.65, 149.57, 145.68, 139.95, 139.92, 137.36, 137.02, 136.92, 136.77, 135.79, 135.68, 133.02, 132.91, 129.57, 129.26, 127.81, 125.26, 124.47, 109.04, 101.23, 87.37, 83.75, 71.08, 62.05, 39.80, 39.52, 37.72, 22.59, 14.36, 11.10, 11.00.

MS (HR-ESI, positive) m/z: $[M+H]^+$ calculated for $C_{28}H_{29}N_5O_5S^+$: 548.1962, found: 548.1972.

5-(4-amino-5-(2-(5-(4-aminophenyl)-2-methylthiophen-3-yl)cyclopent-1-en-1-yl)-6-methyl-7H-pyrrolo[2,3-d]pyrimidin-7-yl)-2-(hydroxymethyl)tetrahydrofuran-3-ol (2^{PhNH_2})

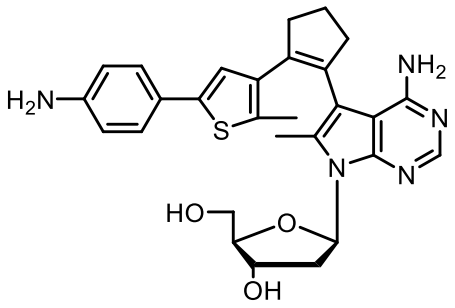

In an Eppendorf vial, **dA^{PhNO_2}** was dissolved in a 2/1 mixture of ethanol and acetic acid. Reduced Iron powder was added and the mixture was placed in the sonicator for 2 h at RT. Then, the mixture was filtered and the filtrate was neutralized by addition of NEt_3 and subsequently purified via HPLC which afforded **dA^{PhNH_2}** as a colourless solid with a yield of 38%.

^{1}H NMR (500 MHz, DMSO-d6) δ 8.25 (d, J = 4.9 Hz, 1H), 7.19 – 7.11 (m, 2H), 6.88 (d, J = 19.0 Hz, 1H), 6.66 (dd, J = 7.9, 3.3 Hz, 2H), 6.43 (dt, J = 24.9, 7.5 Hz, 1H), 4.37 (ddt, J = 25.3, 6.7, 3.2 Hz, 1H), 3.78 (p, J = 4.5 Hz, 1H), 3.65 – 3.56 (m, 1H), 3.55 – 3.45 (m, 1H), 2.97 – 2.82 (m, 2H), 2.80 – 2.71 (m, 1H), 2.70 – 2.57 (m, 2H), 2.18 (d, J = 27.8 Hz, 3H), 2.14 – 2.00 (m, 2H), 1.96 (d, J = 3.8 Hz, 3H).

^{13}C NMR (126 MHz, DMSO-d6) δ 160.68, 158.23, 158.04, 157.20, 154.44, 148.80, 147.44, 142.94, 139.49, 139.22, 135.22, 135.09, 132.37, 131.53, 130.00, 124.27, 121.66, 118.26, 117.44, 115.72, 111.56, 109.53, 100.19, 83.60, 83.32, 70.43, 61.65, 61.47, 39.52, 37.80, 22.46, 15.34, 14.13, 11.34.

MS (HR-ESI, positive) m/z: $[M+H]^+$ calculated for $C_{28}H_{31}N_5O_5SNa^+$: 540.2040, found: 540.2041.

N-benzoyl-N-(5-(2-(5-(3,5-bis(trifluoromethyl)phenyl)-2-methylthiophen-3-yl)cyclopent-1-en-1-yl)-7-4-hydroxy-5-(hydroxymethyl)tetrahydrofuran-2-yl)-6-methyl-7H-pyrrolo[2,3-d]pyrimidin-4-yl)benzamide (3$^{Ph(CF_3)_2}$)

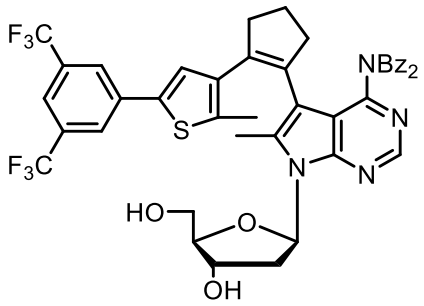

In a Schlenk flask under argon atmosphere, dAPh$(CF_3)_2$ (340 mg,0.53 mmol, 1.00 eq.) was dissolved in anhydrous pyridine (6 mL). At 0°C trimethylsilylchloride (289 mg, 2.66 mmol, 5.00 eq.) was added dropwise and the mixture was stirred 1purified via flash column chromatography (DCM/MeOH (10/1), which yielded the title compound (220 mg, 0.26 mmol, 48%) as a colorless solid.

^{1}H NMR (500 MHz, DMSO-d6) δ 8.47 (d, J = 7.7 Hz, 1H), 7.94 (s, 1H), 7.81 (d, J = 7.6 Hz, 2H), 7.66 (s, 2H), 7.62 (s, 1H), 7.55 (q, J = 7.4 Hz, 2H), 7.42 (dd, J = 38.4, 7.5 Hz, 2H), 7.35 – 7.26 (m, 1H), 7.17 (dt, J = 33.4, 6.3 Hz, 2H), 6.80 (d, J = 43.3 Hz, 1H), 6.56 (dt, J = 85.0, 7.6 Hz, 1H), 5.27 (d, J = 4.4 Hz, 1H), 4.89 (dt, J = 19.4, 5.6 Hz, 1H), 4.39 (ddd, J = 58.3, 6.3, 3.1

Hz, 1H), 3.84 – 3.72 (m, 1H), 3.65 – 3.54 (m, 1H), 3.53 – 3.42 (m, 1H), 2.77 – 2.65 (m, 2H), 2.60 – 2.54 (m, 1H), 2.31 (d, J = 18.8 Hz, 3H), 2.24 (d, J = 12.6 Hz, 3H), 2.17 – 2.03 (m, 2H), 1.83 – 1.70 (m, 1H).

^{13}C NMR (126 MHz, DMSO-d6) δ 173.01, 172.89, 154.05, 153.23, 152.48, 151.82, 138.53, 138.21, 137.94, 137.62, 136.33, 136.18, 135.91, 133.74, 131.83, 131.69, 131.43, 130.65, 129.59, 125.94, 125.93, 122.98, 122.35, 120.82, 112.65, 112.60, 109.79, 109.52, 87.70, 87.42, 84.14, 83.41, 81.44, 71.19, 70.77, 62.13, 61.74, 38.42, 37.99, 22.18, 22.13, 15.62, 15.46, 12.92, 12.01.

MS (HR-ESI, positive) m/z: $[M+H]^+$ calculated for $C_{44}H_{37}F_6N_4O_5S^+$: 743.2112, found: 743.2121.

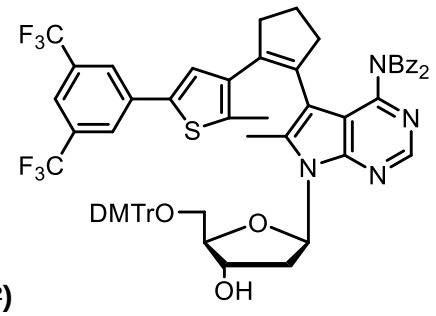

($4^{Ph(CF_3)_2}$) In a Schlenk flask under argon atmosphere, $dAPh(CF_3)_2Bz_2$ (105 mg, 0.124 mmol, 1.00 eq.) and 4-(dimethylamino)pyridine (0.7 mg, 0.05 eq.) were dissolved in anhydrous pyridine (0.5 mL). The solution was cooled to 0°C and dimethoxytritylchloride (53 mg, 0.155 mmol, 1.25 eq.) was added portion wise and the mixture was stirred at RT overnight. purified via flash column chromatography (DCM/MeOH (10/1)), which yielded the title compound (90 mg, 0.08 mmol, 63%) as a yellow solid.

^{1}H NMR (500 MHz, DMSO-d6) δ 8.30 (d, J = 8.6 Hz, 1H), 7.93 (d, J = 7.6 Hz, 1H), 7.80 (dd, J = 13.3, 7.5 Hz, 2H), 7.71 (s, 1H), 7.64 (dd, J = 16.8, 8.8 Hz, 1H), 7.60 (s, 1H), 7.59 – 7.46 (m, 3H), 7.39 (dd, J = 24.7, 7.6 Hz, 2H), 7.28 (d, J = 6.5 Hz, 2H), 7.22 – 7.10 (m, 9H), 6.81 (d, J = 8.1 Hz, 2H), 6.74 (t, J = 10.0 Hz, 3H), 6.67 – 6.58 (m, 1H), 5.34 (dd, J = 10.0, 4.9 Hz, 1H), 4.52 – 4.32 (m, 1H), 3.93 (dt, J = 10.8, 5.4 Hz, 1H), 3.71 – 3.63 (m, 6H), 3.21 – 3.03 (m, 3H), 2.94 – 2.80 (m, 1H), 2.65 – 2.56 (m, 2H), 2.29 (d, J = 38.3 Hz, 3H), 2.19 (d, J = 5.5 Hz, 3H), 2.16 – 2.04 (m, 2H), 1.82 – 1.69 (m, 1H).

^{13}C NMR (126 MHz, DMSO-d6) δ 188.86, 176.30, 171.50, 158.59, 152.90, 151.28, 144.78, 139.02, 137.61, 137.11, 135.86, 135.35, 134.65, 134.39, 134.21, 134.06, 133.21, 132.56, 131.38, 130.82, 129.57, 129.03, 127.62, 127.58, 124.37, 123.84, 122.99, 121.87, 121.39, 113.61, 112.98, 109.48, 84.98, 83.11, 82.95, 69.71, 60.05, 54.97, 54.31, 45.73, 25.16, 21.22, 15.92, 14.94, 11.99, 11.66.

MS (HR-ESI, positive) m/z: $[M+H]^+$ calculated for $C_{65}H_{55}F_6N_4O_7S^+$: 1045.3428, found: 1045.3406.

5-(4-(N-benzoylbenzamido)-5-(2-(5-(3,5-bis(trifluoromethyl)phenyl)-2-methylthiophen-3-yl)cyclopent-1-en-1-yl)-6-methyl-7H-pyrrolo[2,3-d]pyrimidin-7-yl)-2-((bis(4-methoxyphenyl)(phenyl)methoxy)methyl)tetrahydrofuran-3-yl (2-cyanoethyl) diisopropylphosphoramidite ($5^{Ph(CF_3)_2}$)

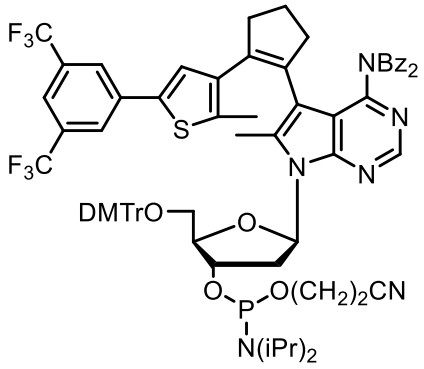

In a Schlenk flask under argon atmosphere, dAPh$(CF_3)_2$Bz$_2$DMT (90 mg, 0.078 mmol, 1.00 eq.) and diisopropylethylamine (20 mg, 0.157 mmol, 2.00 eq.) were dissolved in anhydrous acetonitrile (0.5 mL). 2-cyanoethyl N,N-diisopropylchlorophosphoramidite (24 mg, 0.093 mmol, 1.20 eq.) was added at 0°C and the mixture was stirred at RT for 1 h. Then the mixture was diluted with DCM and the organic phase was washed 3 times with a $NaHCO_3$ (5%) solution, dried over $MgSO_4$, filtered and the solvent was removed under reduced pressure. The title product was obtained as colorless oil and used without further purification.

MS (HR-ESI, positive) m/z: $[M+H]^+$ calculated for $C_{74}H_{72}F_6N_6O_8PS^+$: 1349.4769, found: 1349.4719.

[1]H-NMR spectra

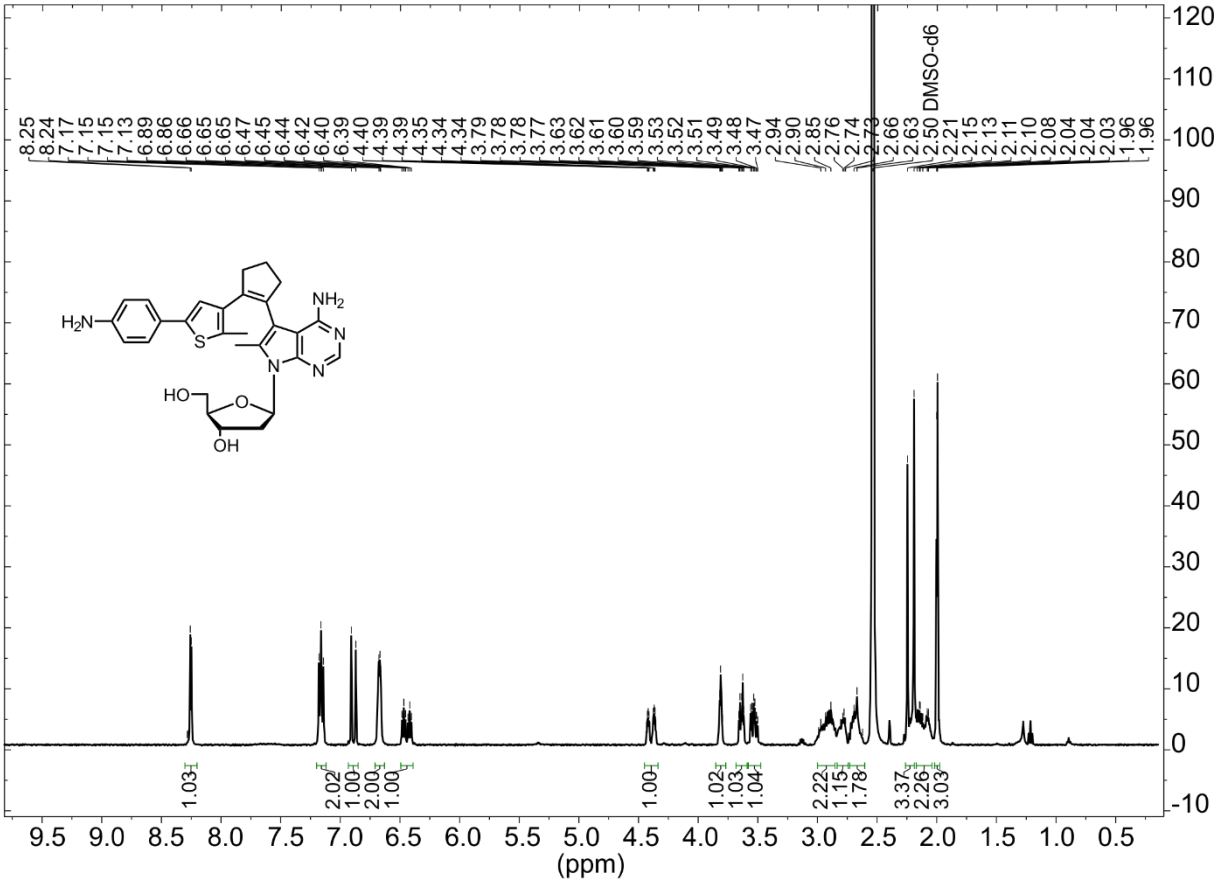

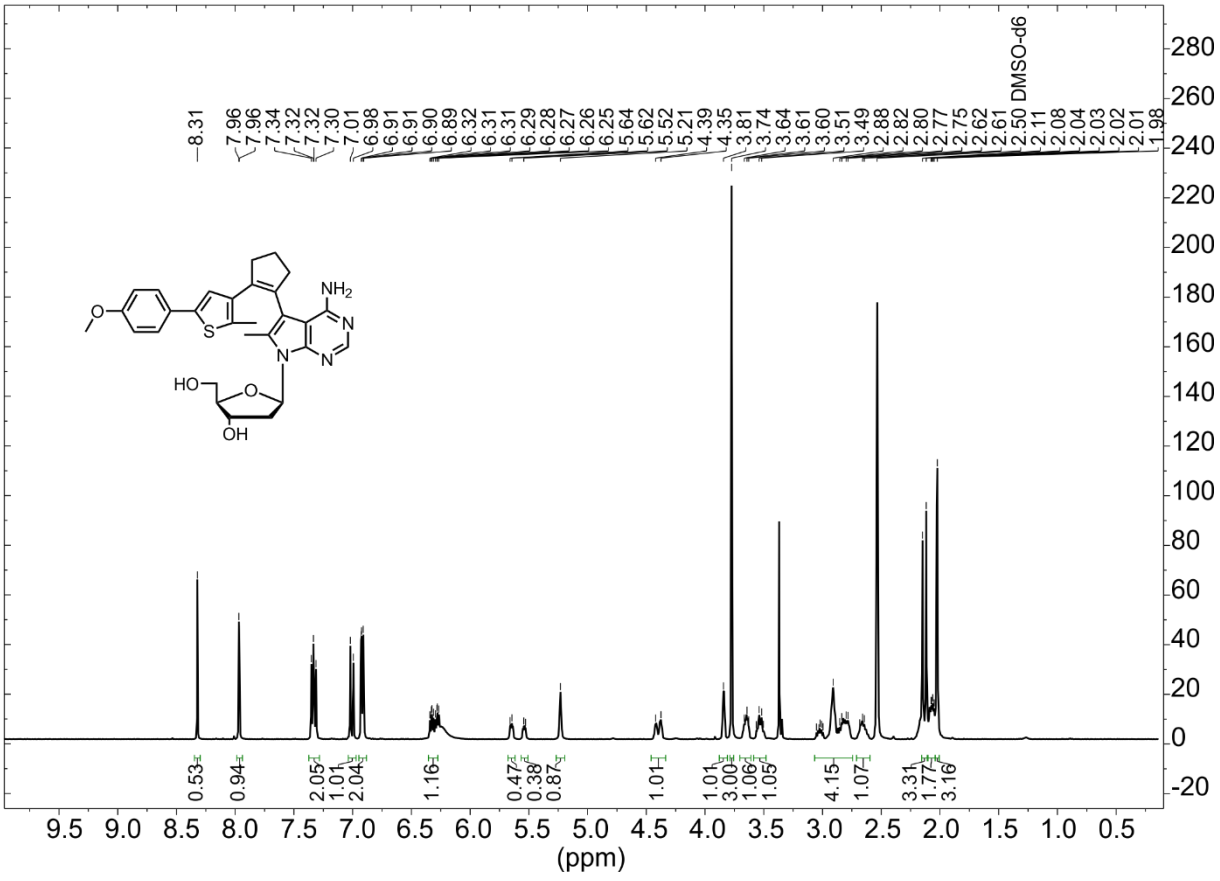

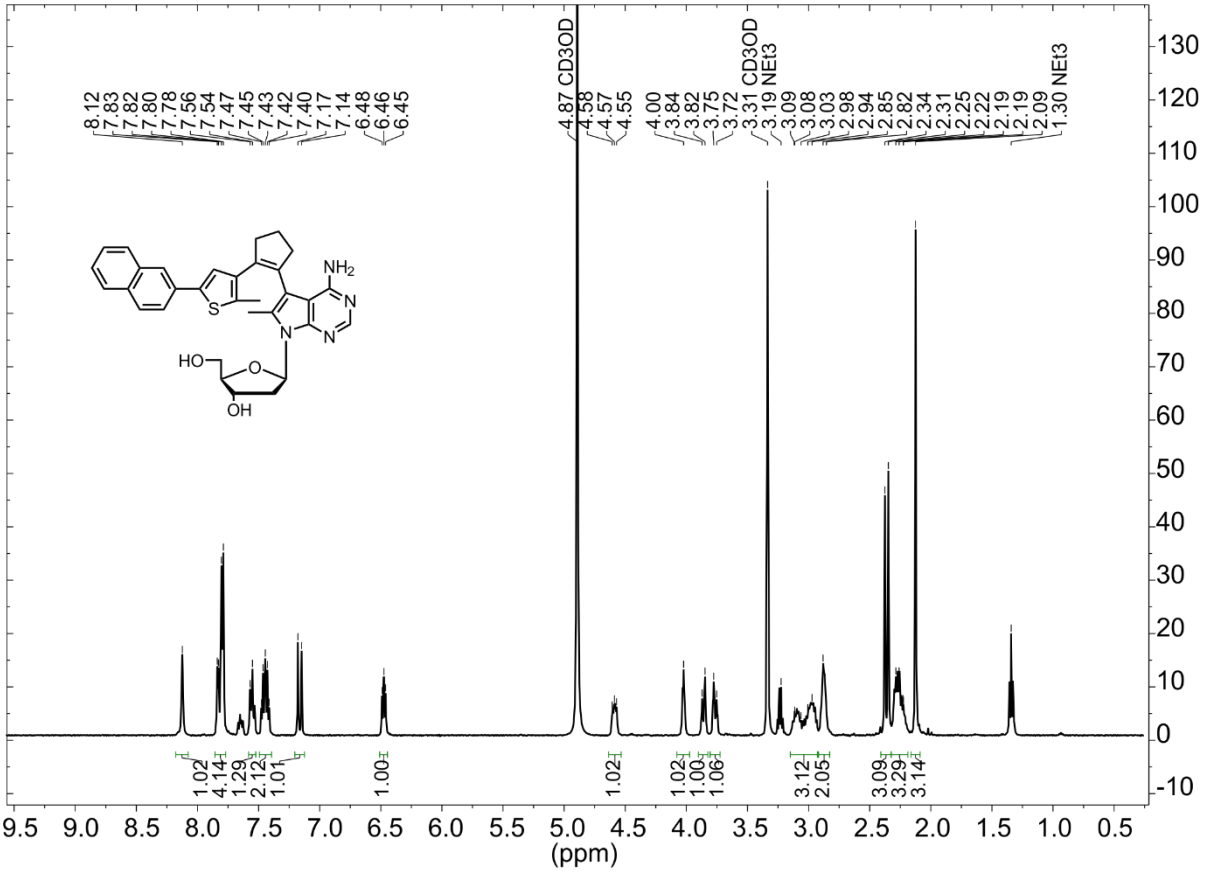
8.12
7.83
7.82
7.80
7.78
7.56
7.54
7.47
7.45
7.43
7.42
7.40
7.17
7.14
6.48
6.46
6.45
4.87 CD3OD
4.58
4.57
4.55
4.00
3.84
3.82
3.75
3.72
3.31 CD3OD
3.19 NEt3
3.09
3.08
3.03
2.98
2.94
2.85
2.82
2.34
2.31
2.25
2.22
2.19
2.09
1.30 NEt3
NH2
N
N
S
N
HO
O
OH
1.02
4.14
1.29
2.12
1.01
1.00
1.02
1.02
1.00
1.06
3.12
2.05
3.09
3.29
3.14
(ppm)

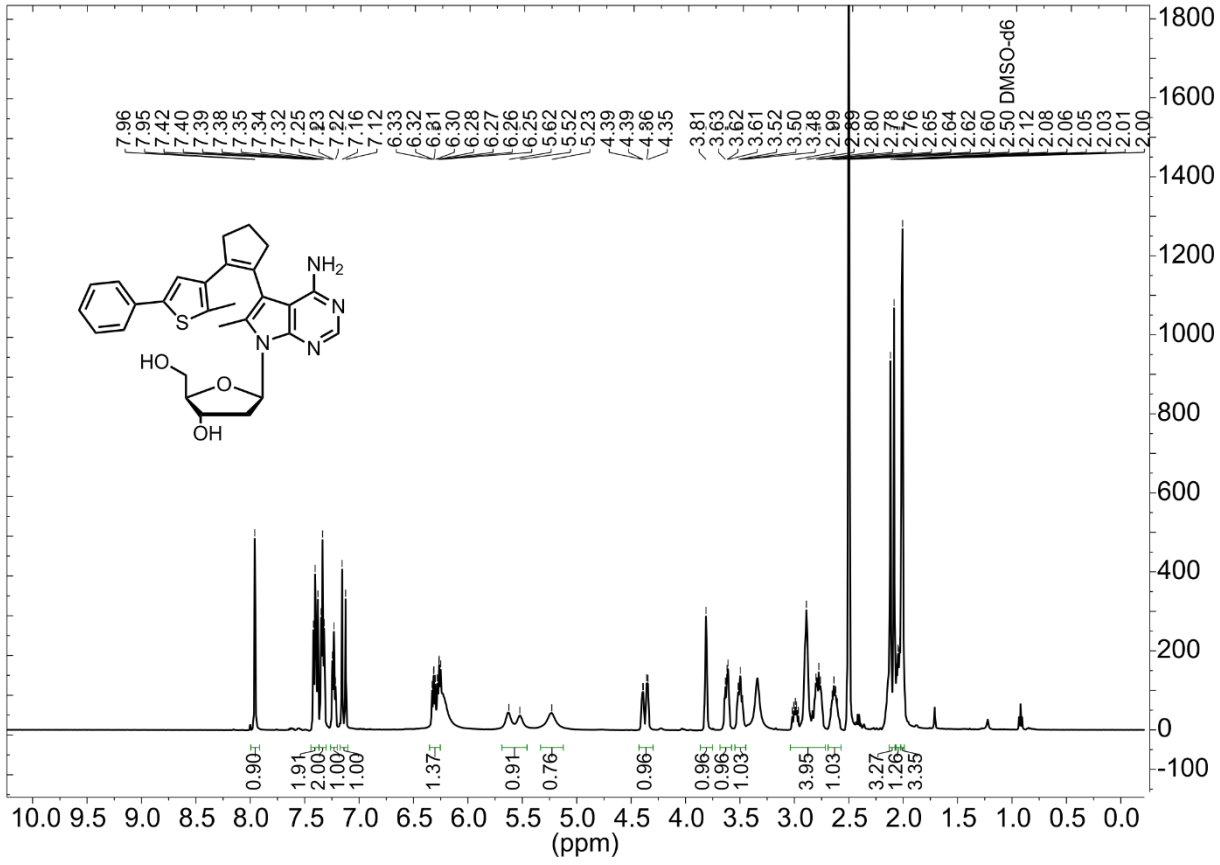
7.96
7.95
7.42
7.40
7.39
7.38
7.35
7.34
7.32
7.25
7.23
7.22
7.16
7.12
6.33
6.32
6.31
6.30
6.28
6.27
6.26
6.25
5.62
5.52
5.23
4.39
4.39
4.36
4.35
3.81
3.63
3.62
3.61
3.52
3.50
3.48
2.89
2.80
2.78
2.76
2.65
2.64
2.62
2.60
2.50 DMSO-d6
2.12
2.08
2.06
2.05
2.03
2.01
2.00
NH2
N
N
S
N
HO
O
OH
0.90
1.91
2.00
1.00
1.00
1.37
0.91
0.76
0.96
0.96
0.96
1.03
3.95
1.03
3.27
1.26
3.35
(ppm)

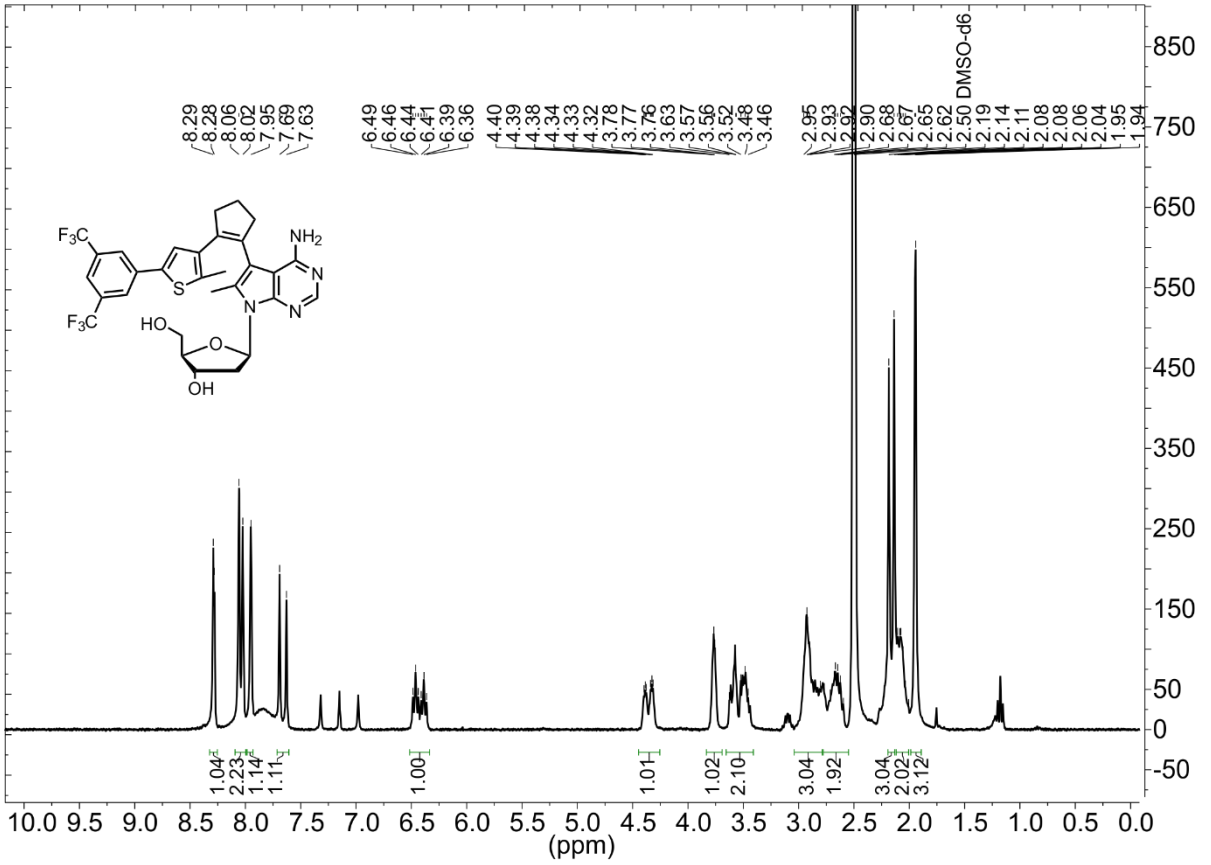
8.29
8.28
8.06
8.02
7.95
7.69
7.63
6.49
6.46
6.44
6.41
6.39
6.36
4.40
4.39
4.38
4.34
4.33
4.32
3.78
3.77
3.76
3.63
3.57
3.56
3.52
3.48
3.46
2.95
2.93
2.92
2.90
2.68
2.67
2.65
2.62
DMSO-d6
2.19
2.14
2.11
2.08
2.08
2.06
2.04
1.95
1.94
F3C
F3C
NH2
S
N
N
N
HO
O
OH
1.04
2.23
1.14
1.11
1.00
1.01
1.02
2.10
3.04
1.92
3.04
2.02
3.12
(ppm)

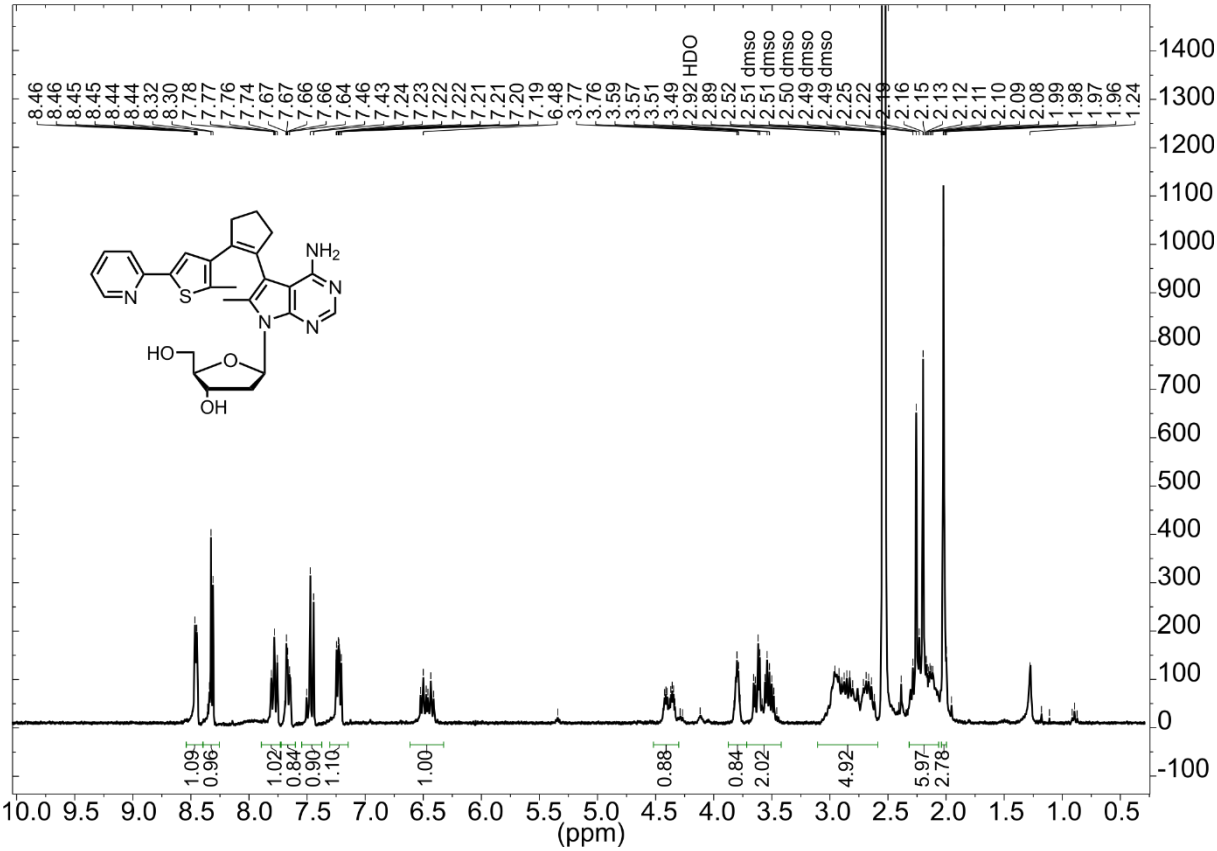
8.46
8.46
8.45
8.45
8.44
8.44
8.32
8.30
7.78
7.77
7.76
7.74
7.67
7.67
7.66
7.66
7.64
7.46
7.43
7.24
7.23
7.22
7.22
7.21
7.21
7.20
7.19
6.48
3.77
3.76
3.59
3.57
3.51
3.49
2.92
HDO
2.89
2.52
dmso
2.51
dmso
2.50
dmso
2.49
dmso
2.25
2.22
2.16
2.15
2.13
2.12
2.11
2.10
2.09
2.08
1.99
1.98
1.97
1.96
1.24
NH2
N
S
N
N
N
HO
O
OH
1.09
0.96
1.02
0.84
0.90
1.10
1.00
0.88
0.84
2.02
4.92
5.97
2.78
(ppm)

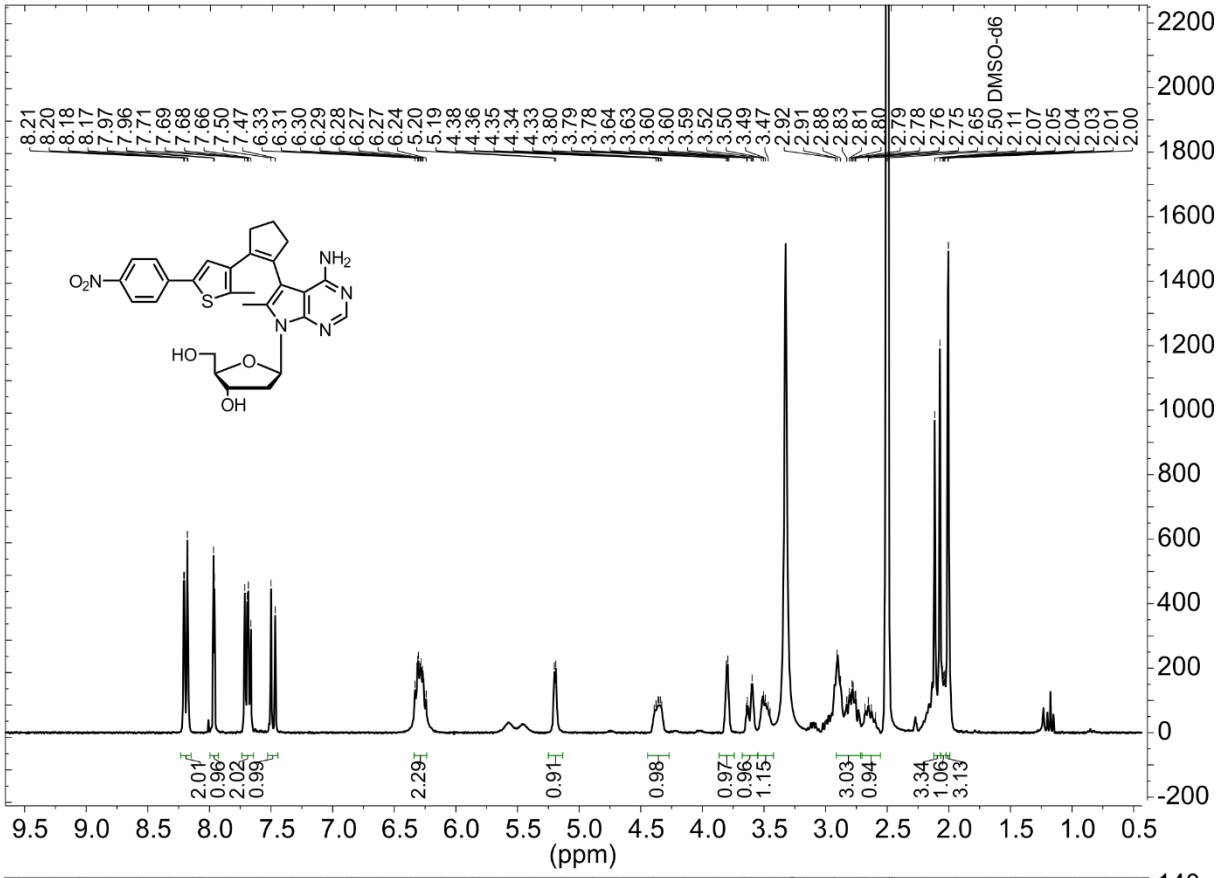
DMSO-d6
(ppm)

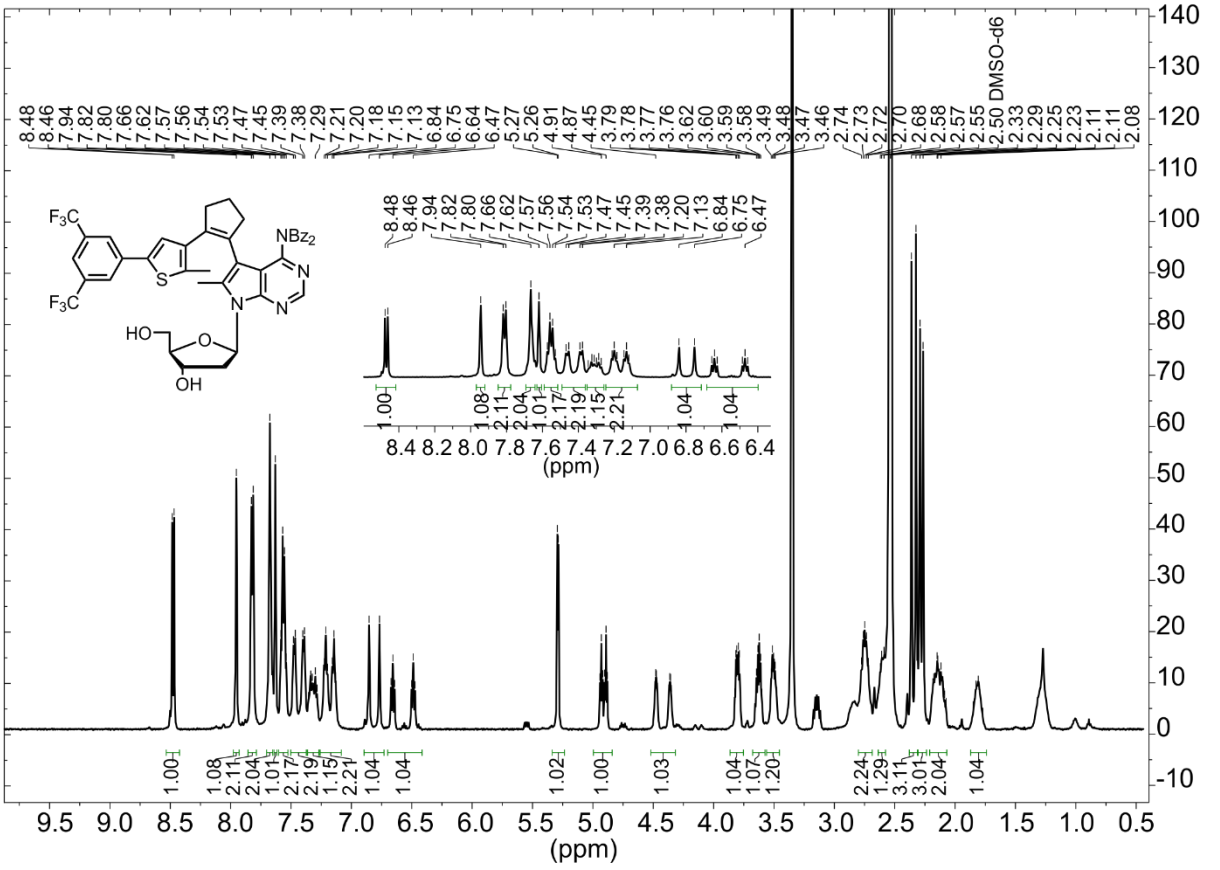
DMSO-d6
(ppm)
(ppm)

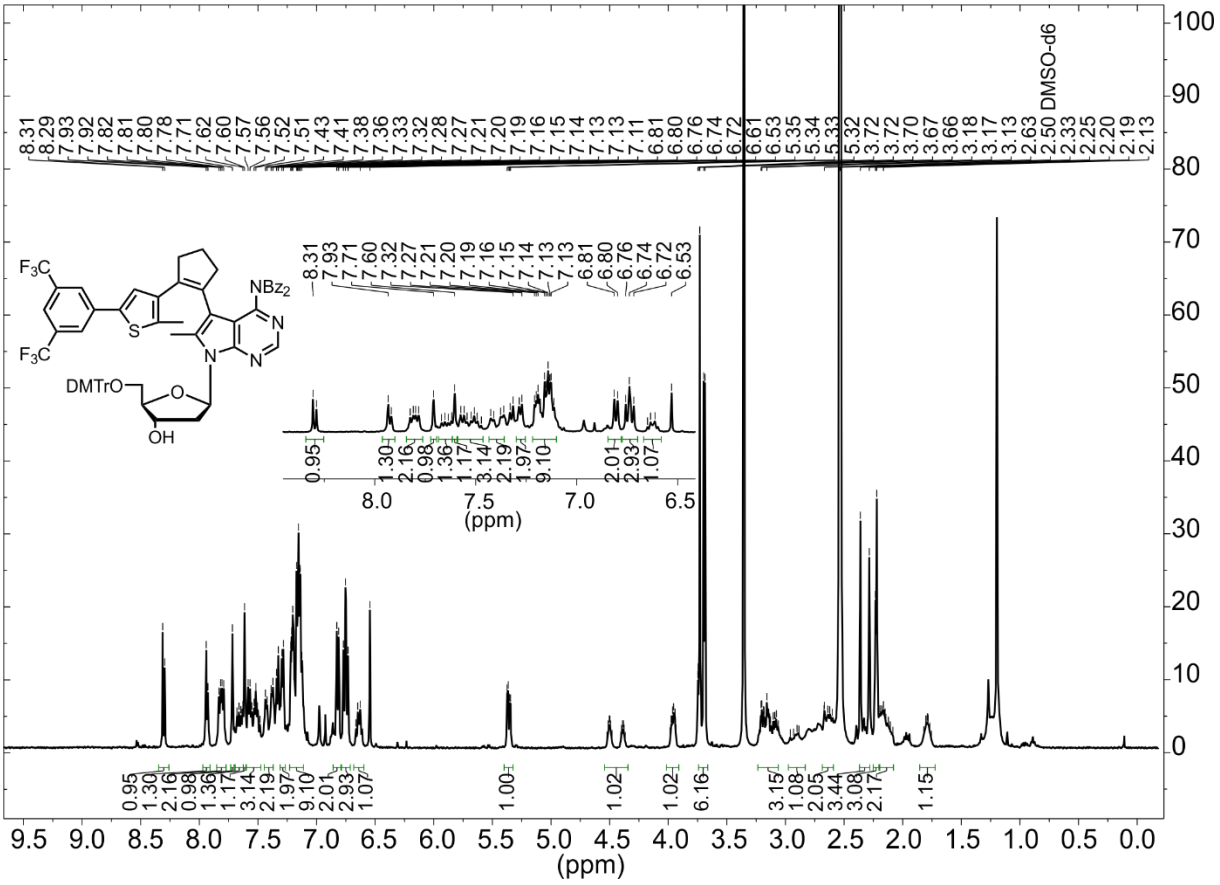
DMSO-d6
(ppm)

Shutter files

Cyclization: dA^{PhNH_2}

```
#1 Protocol QYDS measurement
#2 Date:        12/18/2020
#3 Sample:      dA_Ph_NH2_OC
#4 Researcher:  Simon
#5 LED:         4 NIKKISO VPC1A1 300 nm
#6 Filter::
#7 Solar Cell:  HV-00X
#8 Voltage after reference cuvette (V): X.XX, High Power range (A)
#9 Calibration Factor (mW/V):           0.374
#10 Power after reference cuvette (mW): 0.308
#11 Insert comments below, do not change the header up to here
```

Number	TimeStart	TimeEnd	Runtime	Illum.-Time	Power(mW)	Cell (mW)	Voltage(V)	Current(A)
0	10:32:42.407	10:32:42.407	0.000	0.000	0.000	0.027	0.000	0.000
1	11:05:13.043	11:06:13.418	60.318	60.318	0.018	0.032	5.320	0.150
2	11:07:26.757	11:08:33.394	66.654	126.972	0.022	0.037	5.320	0.150
3	11:09:47.517	11:11:01.081	73.575	200.547	0.025	0.039	5.320	0.150
4	11:12:13.870	11:13:34.483	80.502	281.049	0.029	0.042	5.320	0.150
5	11:14:50.958	11:16:19.617	88.736	369.785	0.032	0.045	5.320	0.150
6	11:17:36.195	11:19:14.028	97.817	467.602	0.028	0.046	5.320	0.150
7	11:20:31.173	11:22:19.295	108.097	575.699	0.035	0.048	5.320	0.150
8	11:23:38.679	11:25:37.200	118.598	694.297	0.037	0.052	5.320	0.150
9	11:26:52.702	11:29:03.287	130.671	824.968	0.040	0.054	5.320	0.150
10	11:30:16.855	11:32:40.420	143.521	968.489	0.043	0.055	5.320	0.150
11	11:33:55.003	11:36:32.859	157.805	1126.294	0.046	0.056	5.320	0.150
12	11:37:53.139	11:40:47.110	173.916	1300.210	0.049	0.057	5.320	0.150
13	11:42:04.260	11:45:15.895	191.541	1491.751	0.041	0.058	5.320	0.150
14	11:46:29.344	11:50:00.105	210.671	1702.422	0.038	0.058	5.320	0.150

Cycloreversion: dA^{PhNH_2}

```
#1 Protocol QYDS measurement
#2 Date:        12/18/2020
#3 Sample:      dA_Ph_NH2_CO
#4 Researcher:  Simon
#5 LED:         13 OSRAM LVCK7P-JYKZ 508 nm
#6 Filter::
#7 Solar Cell:  HV-00X
#8 Voltage after reference cuvette (V): X.XX, High Power range (A)
#9 Calibration Factor (mW/V):           0.132
#10 Power after reference cuvette (mW): 0.653
#11 Insert comments below, do not change the header up to here
```

Number	TimeStart	TimeEnd	Runtime	Illum.-Time	Power(mW)	Cell (mW)	Voltage(V)	Current(A)
0	12:04:46.181	12:04:46.181	0.000	0.000	-0.003	0.165	3.090	0.099
1	12:51:26.620	12:52:29.342	62.731	62.731	-0.003	0.201	3.100	0.099
2	12:53:42.813	12:54:50.247	67.516	130.247	-0.002	0.236	3.110	0.099
3	12:56:01.256	12:57:14.718	73.574	203.821	-0.000	0.276	3.110	0.099
4	12:58:35.225	12:59:56.173	80.786	284.607	-0.002	0.320	3.110	0.099
5	13:01:08.844	13:02:37.631	88.664	373.271	0.002	0.375	3.110	0.099
6	13:03:52.330	13:05:30.177	97.771	471.042	-0.001	0.429	3.100	0.099
7	13:06:44.869	13:08:32.759	107.867	578.909	0.004	0.484	3.110	0.099
8	13:09:46.781	13:11:45.534	118.733	697.642	0.001	0.530	3.100	0.099
9	13:13:06.601	13:15:17.422	130.823	828.465	-0.002	0.569	3.100	0.099
10	13:16:33.671	13:18:57.572	143.879	972.344	-0.001	0.599	3.100	0.099
11	13:20:23.668	13:23:01.764	157.981	1130.325	0.002	0.620	3.100	0.099
12	13:24:15.896	13:27:09.979	173.893	1304.218	0.003	0.632	3.100	0.099
13	13:28:36.635	13:31:48.286	191.575	1495.793	0.006	0.640	3.110	0.099
14	13:33:02.877	13:36:33.993	211.043	1706.836	-0.000	0.644	3.100	0.099

Cyclization: dA^{PhOMe}

```
#1 Protocol QYDS measurement
#2 Date:        12/13/2020
#3 Sample:      dA_An_OC
#4 Researcher:  Simon
#5 LED:         4 NIKKISO VPC1A1 300 nm
#6 Filter::
#7 Solar Cell:  HV-00X
#8 Voltage after reference cuvette (V): X.XX, High Power range (A)
#9 Calibration Factor (mW/V):           0.374
#10 Power after reference cuvette (mW): 0.221
#11 Insert comments below, do not change the header up to here
```

Number	TimeStart	TimeEnd	Runtime	Illum.-Time	Power(mW)	Cell (mW)	Voltage(V)	Current(A)
0	11:31:42.512	11:31:42.512	0.000	0.000	0.000	0.014	0.000	0.000
1	11:37:23.864	11:38:24.481	60.682	60.682	0.004	0.015	5.210	0.109
2	11:39:38.703	11:40:45.659	66.960	127.642	0.005	0.016	5.210	0.109
3	11:42:03.140	11:43:16.722	73.467	201.109	0.006	0.017	5.210	0.109
4	11:44:32.074	11:45:52.794	80.582	281.691	0.005	0.017	5.210	0.109
5	11:47:08.250	11:48:37.015	88.792	370.483	0.005	0.018	5.220	0.109
6	11:49:53.029	11:51:30.962	97.857	468.340	0.008	0.018	5.210	0.109
7	11:52:44.970	11:54:33.289	108.383	576.723	0.008	0.018	5.210	0.109
8	11:55:53.663	11:57:52.166	118.507	695.230	0.006	0.018	5.210	0.109
9	11:59:06.287	12:01:16.865	130.550	825.780	0.006	0.018	5.210	0.109
10	12:02:52.999	12:05:16.431	143.517	969.297	0.007	0.018	5.210	0.109
11	12:09:32.675	12:12:10.416	157.731	1127.028	-0.001	0.018	5.210	0.109
12	12:13:31.704	12:16:25.547	173.857	1300.885	0.002	0.018	5.210	0.109
13	12:17:45.025	12:20:56.634	191.541	1492.426	0.004	0.018	5.210	0.109
14	12:22:12.325	12:25:43.281	210.794	1703.220	0.006	0.019	5.210	0.109

Cycloreversion: dA^{PhOMe}

#1 Protocol QYDS measurement
#2 Date: 12/14/2020
#3 Sample: dA_An_CO
#4 Researcher: Simon
#5 LED: 13 OSRAM LVCK7P-JYKZ 508 nm
#6 Filter::
#7 Solar Cell: HV-00X
#8 Voltage after reference cuvette (V): X.XX, High Power range (A)
#9 Calibration Factor (mW/V): 0.132
#10 Power after reference cuvette (mW): 0.775
#11 Insert comments below, do not change the header up to here

Number	TimeStart	TimeEnd	Runtime	Illum.-Time	Power(mW)	Cell (mW)	Voltage(V)	Current(A)
0	12:54:14.183	12:54:14.183	0.000	0.000	0.000	0.191	0.000	0.000
1	14:38:44.406	14:39:44.897	60.578	60.578	-0.013	0.258	3.110	0.099
2	14:41:03.276	14:42:09.908	66.443	127.021	-0.014	0.325	3.110	0.099
3	14:43:23.703	14:44:37.273	73.673	200.694	-0.014	0.402	3.110	0.099
4	14:45:50.285	14:47:10.894	80.675	281.369	-0.016	0.496	3.100	0.099
5	14:48:25.817	14:49:54.596	88.688	370.057	-0.011	0.579	3.100	0.099
6	14:51:11.632	14:52:49.579	97.912	467.969	-0.013	0.646	3.110	0.099
7	14:54:07.280	14:55:55.182	107.876	575.845	-0.013	0.700	3.110	0.099
8	14:57:11.556	14:59:10.302	118.654	694.499	-0.012	0.734	3.100	0.099
9	15:00:24.764	15:02:35.470	130.589	825.088	-0.008	0.756	3.110	0.099
10	15:03:51.837	15:06:15.625	143.606	968.694	-0.012	0.764	3.100	0.099
11	15:07:33.440	15:10:11.203	157.729	1126.423	-0.009	0.769	3.110	0.099
12	15:11:29.250	15:14:22.878	173.712	1300.135	-0.011	0.769	3.110	0.099

Cyclization: dA^{Np}

#1 Protocol QYDS measurement
#2 Date: 12/13/2020
#3 Sample: dA_Np_OC
#4 Researcher: Simon
#5 LED: 4 NIKKISO VPC1A1 300 nm
#6 Filter::
#7 Solar Cell: HV-00X
#8 Voltage after reference cuvette (V): X.XX, High Power range (A)
#9 Calibration Factor (mW/V): 0.374
#10 Power after reference cuvette (mW): 0.241
#11 Insert comments below, do not change the header up to here

Number	TimeStart	TimeEnd	Runtime	Illum.-Time	Power(mW)	Cell (mW)	Voltage(V)	Current(A)
0	10:24:48.598	10:24:48.598	0.000	0.000	0.000	0.043	0.000	0.000
1	10:50:36.483	10:51:36.959	60.516	60.516	0.043	0.047	5.240	0.120
2	10:52:52.532	10:53:59.278	66.746	127.262	0.047	0.051	5.240	0.120
3	10:55:13.622	10:56:27.184	73.502	200.764	0.053	0.053	5.240	0.120
4	10:57:42.088	10:59:02.705	80.611	281.375	0.055	0.055	5.240	0.120
5	11:00:19.404	11:01:48.393	89.043	370.418	0.056	0.057	5.240	0.120
6	11:03:04.193	11:04:41.776	97.527	467.945	0.060	0.059	5.240	0.120
7	11:05:58.905	11:07:46.563	107.663	575.608	0.061	0.059	5.240	0.120
8	11:09:01.568	11:11:00.302	118.630	694.238	0.061	0.059	5.240	0.120
9	11:12:18.445	11:14:29.131	130.576	824.814	0.063	0.059	5.240	0.120
10	11:15:43.356	11:18:07.124	143.613	968.427	0.062	0.059	5.240	0.120
11	11:19:32.422	11:22:10.155	157.801	1126.228	0.060	0.059	5.240	0.120

Cycloreversion: dA^{Np}

#1 Protocol QYDS measurement
#2 Date: 12/14/2020
#3 Sample: dA_Np_CO
#4 Researcher: Simon
#5 LED: 13 OSRAM LVCK7P-JYKZ 508 nm
#6 Filter::
#7 Solar Cell: HV-00X
#8 Voltage after reference cuvette (V): X.XX, High Power range (A)
#9 Calibration Factor (mW/V): 0.132
#10 Power after reference cuvette (mW): 0.775
#11 Insert comments below, do not change the header up to here

Number	TimeStart	TimeEnd	Runtime	Illum.-Time	Power(mW)	Cell (mW)	Voltage(V)	Current(A)
0	11:56:39.573	11:56:39.573	0.000	0.000	0.000	0.236	0.000	0.000
1	12:15:57.070	12:16:57.451	60.333	60.333	-0.005	0.307	3.110	0.099
2	12:18:15.598	12:19:22.225	66.510	126.843	-0.003	0.378	3.110	0.099
3	12:20:39.253	12:21:52.831	73.589	200.432	-0.005	0.449	3.100	0.099
4	12:23:08.189	12:24:28.918	80.637	281.069	-0.006	0.529	3.110	0.099
5	12:25:55.792	12:27:24.673	88.715	369.784	-0.007	0.593	3.110	0.099
6	12:28:38.581	12:30:16.305	97.672	467.456	-0.007	0.653	3.110	0.099
7	12:31:33.901	12:33:21.682	107.789	575.245	-0.006	0.701	3.110	0.099
8	12:34:42.409	12:36:41.256	118.847	694.092	-0.006	0.734	3.100	0.099
9	12:37:59.628	12:40:09.999	130.355	824.447	-0.005	0.755	3.110	0.099
10	12:41:31.056	12:43:54.744	143.593	968.040	-0.009	0.765	3.110	0.099
11	12:45:16.372	12:47:54.251	157.746	1125.786	-0.008	0.769	3.110	0.099
12	12:49:29.846	12:52:23.600	173.767	1299.553	-0.006	0.769	3.110	0.099

Cyclization: dA^{Ph}

#1 Protocol QYDS measurement
#2 Date: 12/11/2020
#3 Sample: dA_Ph_OC
#4 Researcher: Simon
#5 LED: 4 NIKKISO VPC1A1 300 nm
#6 Filter::
#7 Solar Cell: HV-00X
#8 Voltage after reference cuvette (V): X.XX, High Power range (A)
#9 Calibration Factor (mW/V): 0.374
#10 Power after reference cuvette (mW): 0.241
#11 Insert comments below, do not change the header up to here

Number	TimeStart	TimeEnd	Runtime	Illum.-Time	Power(mW)	Cell (mW)	Voltage(V)	Current(A)
0	13:01:25.324	13:01:25.324	0.000	0.000	0.000	0.034	0.000	0.000
1	15:16:30.303	15:17:31.000	60.772	60.772	0.036	0.039	5.240	0.120
2	15:18:46.015	15:19:52.877	66.807	127.579	0.043	0.044	5.250	0.120
3	15:22:36.097	15:23:49.544	73.432	201.011	0.038	0.049	5.240	0.120
4	15:25:04.342	15:26:25.059	80.708	281.719	0.037	0.054	5.240	0.120
5	15:27:41.867	15:29:10.637	88.684	370.403	0.038	0.059	5.240	0.120
6	15:30:52.933	15:32:30.868	97.802	468.205	0.036	0.062	5.240	0.120
7	15:33:46.215	15:35:33.987	107.659	575.864	0.034	0.065	5.240	0.120
8	15:36:56.281	15:38:55.034	118.592	694.456	0.035	0.065	5.240	0.120
9	15:40:19.323	15:42:30.033	130.526	824.982	0.032	0.066	5.240	0.120
10	15:43:56.906	15:46:20.519	143.332	968.314	0.034	0.066	5.240	0.120
11	15:47:40.573	15:50:18.325	157.585	1125.899	0.030	0.067	5.240	0.120

Cycloreversion: dA^{Ph}

#1 Protocol QYDS measurement
#2 Date: 12/14/2020
#3 Sample: dA_PH_CO
#4 Researcher: Simon
#5 LED: 13 OSRAM LVCK7P-JYKZ 508 nm
#6 Filter::
#7 Solar Cell: HV-00X
#8 Voltage after reference cuvette (V): X.XX, High Power range (A)
#9 Calibration Factor (mW/V): 0.132
#10 Power after reference cuvette (mW): 0.910
#11 Insert comments below, do not change the header up to here

Number	TimeStart	TimeEnd	Runtime	Illum.-Time	Power(mW)	Cell (mW)	Voltage(V)	Current(A)
0	08:47:06.076	08:47:06.076	0.000	0.000	0.039	0.278	0.000	0.000
1	11:22:19.779	11:23:20.268	60.506	60.506	0.041	0.377	3.110	0.099
2	11:24:33.506	11:25:40.042	66.488	126.994	0.043	0.476	3.110	0.099
3	11:26:55.727	11:28:09.413	73.634	200.628	0.042	0.590	3.110	0.099
4	11:29:28.570	11:30:49.624	81.029	281.657	0.044	0.687	3.110	0.099
5	11:32:05.534	11:33:34.185	88.708	370.365	0.046	0.780	3.110	0.099
6	11:34:52.787	11:36:30.506	97.659	468.024	0.044	0.829	3.110	0.099
7	11:37:47.190	11:39:35.013	107.859	575.883	0.047	0.872	3.110	0.099
8	11:40:50.480	11:42:49.097	118.580	694.463	0.048	0.887	3.110	0.099
9	11:44:05.559	11:46:16.261	130.577	825.040	0.049	0.898	3.110	0.099
10	11:47:35.303	11:49:58.856	143.458	968.498	0.049	0.900	3.110	0.099
11	11:51:19.800	11:53:57.650	157.749	1126.247	0.049	0.900	3.110	0.099

Cyclization: dA^{2Py}

#1 Protocol QYDS measurement
#2 Date: 12/10/2020
#3 Sample: dA_Ph_2Py_300nm
#4 Researcher: Simon
#5 LED: 4 NIKKISO VPC1A1 300 nm
#6 Filter::
#7 Solar Cell: HV-00X
#8 Voltage after reference cuvette (V): X.XX, High Power range (A)
#9 Calibration Factor (mW/V): 0.374
#10 Power after reference cuvette (mW): 0.436
#11 Insert comments below, do not change the header up to here

Number	TimeStart	TimeEnd	Runtime	Illum.-Time	Power(mW)	Cell (mW)	Voltage(V)	Current(A)
0	12:51:01.640	12:51:01.640	0.000	0.000	0.000	0.052	0.000	0.000
1	13:02:08.447	13:03:08.822	60.248	60.248	0.003	0.059	5.180	0.099
2	13:04:22.295	13:05:29.048	66.669	126.917	0.002	0.066	5.180	0.099
3	13:07:07.885	13:08:21.462	73.515	200.432	0.002	0.072	5.180	0.099
4	13:09:36.486	13:10:56.886	80.344	280.776	0.003	0.079	5.180	0.099
5	13:12:21.303	13:13:50.090	88.760	369.536	0.004	0.086	5.180	0.099
6	13:15:04.007	13:16:41.842	97.715	467.251	0.002	0.092	5.180	0.099
7	13:17:55.524	13:19:43.305	107.619	574.870	0.002	0.095	5.180	0.099
8	13:21:26.951	13:23:25.797	118.720	693.590	0.002	0.099	5.180	0.099
9	13:24:59.495	13:27:10.084	130.474	824.064	0.005	0.099	5.180	0.099
10	13:28:23.763	13:30:47.769	143.945	968.009	0.003	0.100	5.180	0.099
11	13:32:28.058	13:35:05.829	157.647	1125.656	0.004	0.101	5.180	0.099
12	13:36:43.556	13:39:37.543	173.860	1299.516	0.000	0.102	5.180	0.099
13	13:40:52.450	13:44:03.978	191.418	1490.934	-0.001	0.103	5.180	0.099

Cycloreversion: dA^{2Py}

#1 Protocol QYDS measurement
#2 Date: 12/10/2020
#3 Sample: dA_Ph_2Py_505nm
#4 Researcher: Simon
#5 LED: 13 OSRAM LVCK7P-JYKZ 508 nm
#6 Filter::
#7 Solar Cell: HV-00X
#8 Voltage after reference cuvette (V): X.XX, High Power range (A)
#9 Calibration Factor (mW/V): 0.132
#10 Power after reference cuvette (mW): 2.173
#11 Insert comments below, do not change the header up to here

Number	TimeStart	TimeEnd	Runtime	Illum.-Time	Power(mW)	Cell (mW)	Voltage(V)	Current(A)
0	13:55:17.749	13:55:17.749	0.000	0.000	0.000	0.410	0.000	0.000
1	15:09:33.694	15:10:33.947	60.209	60.209	-0.001	0.539	3.230	0.200
2	15:13:03.870	15:14:10.275	66.363	126.572	-0.006	0.668	3.230	0.200
3	15:16:36.632	15:17:49.970	73.449	200.021	-0.008	0.796	3.220	0.200
4	15:19:08.456	15:20:29.052	80.454	280.475	-0.008	0.983	3.230	0.200
5	15:21:43.403	15:23:12.616	89.087	369.562	-0.010	1.174	3.230	0.200
6	15:25:58.970	15:27:37.346	98.370	467.932	-0.010	1.375	3.230	0.200
7	15:28:53.820	15:30:41.939	108.019	575.951	-0.006	1.590	3.230	0.200
8	15:32:02.433	15:34:01.388	118.765	694.716	-0.007	1.783	3.230	0.200
9	15:35:20.658	15:37:31.454	130.780	825.496	-0.007	1.931	3.230	0.200
10	15:38:47.811	15:41:11.805	143.922	969.418	-0.005	2.028	3.230	0.200
11	15:42:33.979	15:45:11.830	157.806	1127.224	-0.010	2.099	3.220	0.200
12	15:47:02.834	15:49:56.666	173.808	1301.032	-0.012	2.129	3.230	0.200
13	15:51:34.711	15:54:46.554	191.766	1492.798	-0.011	2.159	3.230	0.200
14	15:56:50.981	16:00:21.851	210.761	1703.559	-0.013	2.169	3.220	0.200

Cyclization: $dA^{Ph(CF_3)2}$

#1 Protocol QYDS measurement
#2 Date: 12/13/2020
#3 Sample: dA_PH_CF3_OC
#4 Researcher: Simon
#5 LED: 4 NIKKISO VPC1A1 300 nm
#6 Filter::
#7 Solar Cell: HV-00X
#8 Voltage after reference cuvette (V): X.XX, High Power range (A)
#9 Calibration Factor (mW/V): 0.374
#10 Power after reference cuvette (mW): 0.205
#11 Insert comments below, do not change the header up to here

Number	TimeStart	TimeEnd	Runtime	Illum.-Time	Power(mW)	Cell (mW)	Voltage(V)	Current(A)
0	12:54:30.983	12:54:30.983	0.000	0.000	0.000	0.026	0.000	0.000
1	13:04:57.287	13:05:57.659	60.392	60.392	0.004	0.032	5.180	0.099
2	13:07:12.353	13:08:18.986	66.710	127.102	0.004	0.038	5.180	0.099
3	13:09:34.684	13:10:48.140	73.460	200.562	0.005	0.044	5.180	0.099
4	13:12:03.938	13:13:24.547	80.548	281.110	0.006	0.051	5.180	0.099
5	13:14:38.450	13:16:07.215	88.665	369.775	0.007	0.058	5.180	0.099
6	13:17:22.789	13:19:00.739	97.845	467.620	0.007	0.062	5.180	0.099
7	13:20:16.204	13:22:04.093	107.806	575.426	0.009	0.067	5.180	0.099
8	13:23:19.332	13:25:18.063	118.643	694.069	0.009	0.069	5.180	0.099
9	13:26:34.195	13:28:44.898	130.729	824.798	0.009	0.072	5.180	0.099
10	13:30:13.348	13:32:37.023	143.542	968.340	0.008	0.072	5.180	0.099
11	13:33:52.608	13:36:30.487	157.827	1126.167	0.008	0.073	5.180	0.099

Cycloreversion: $dA^{Ph(CF_3)2}$

#1 Protocol QYDS measurement
#2 Date: 12/16/2020
#3 Sample: dA_Ph_CF3_CO
#4 Researcher: Simon
#5 LED: 13 OSRAM LVCK7P-JYKZ 508 nm
#6 Filter::
#7 Solar Cell: HV-00X
#8 Voltage after reference cuvette (V): X.XX, High Power range (A)
#9 Calibration Factor (mW/V): 0.132
#10 Power after reference cuvette (mW): 2.125
#11 Insert comments below, do not change the header up to here

Number	TimeStart	TimeEnd	Runtime	Illum.-Time	Power(mW)	Cell (mW)	Voltage(V)	Current(A)
0	10:21:47.987	10:21:47.987	0.000	0.000	0.000	0.379	0.000	0.000
1	10:40:39.747	10:41:40.456	60.715	60.715	0.008	0.491	3.100	0.099
2	10:42:59.721	10:44:06.469	66.702	127.417	0.008	0.603	3.110	0.099
3	10:45:21.046	10:46:34.839	73.686	201.103	0.005	0.743	3.100	0.099
4	10:47:52.326	10:49:13.159	80.618	281.721	0.005	0.891	3.100	0.099
5	10:50:30.872	10:51:59.862	89.051	370.772	0.006	1.079	3.110	0.099
6	10:53:12.858	10:54:50.573	97.576	468.348	0.006	1.283	3.110	0.099
7	10:56:04.815	10:57:52.921	108.219	576.567	0.004	1.505	3.110	0.099
8	10:59:14.770	11:01:13.393	118.548	695.115	0.004	1.683	3.110	0.099
9	11:02:29.876	11:04:40.469	130.542	825.657	0.012	1.766	3.100	0.099
10	11:05:57.622	11:08:21.292	143.642	969.299	0.014	1.943	3.100	0.099
11	11:09:49.172	11:12:27.034	157.783	1127.082	0.017	2.023	3.100	0.099
12	11:13:44.518	11:16:37.460	172.797	1299.879	0.017	2.069	3.100	0.099
13	11:17:52.929	11:21:04.560	191.499	1491.378	0.019	2.091	3.100	0.099
14	11:22:22.490	11:25:53.678	211.167	1702.545	0.016	2.114	3.110	0.099

Cycloreversion: dA^{Pym}

#1 Protocol QYDS measurement
#2 Date: 12/16/2020
#3 Sample: dA_Pym_CO
#4 Researcher: Simon
#5 LED: 13 OSRAM LVCK7P-JYKZ 508 nm
#6 Filter::
#7 Solar Cell: HV-00X
#8 Voltage after reference cuvette (V): X.XX, High Power range (A)
#9 Calibration Factor (mW/V): 0.132
#10 Power after reference cuvette (mW): 4.508
#11 Insert comments below, do not change the header up to here

Number	TimeStart	TimeEnd	Runtime	Illum.-Time	Power(mW)	Cell (mW)	Voltage(V)	Current(A)
0	07:32:45.823	07:32:45.823	0.000	0.000	0.000	1.272	0.000	0.000
1	08:57:30.711	08:58:31.198	60.514	60.514	0.045	1.530	3.220	0.200
2	08:59:49.805	09:00:56.547	66.666	127.180	0.044	1.788	3.220	0.200
3	09:02:11.120	09:03:24.796	73.654	200.834	0.045	2.099	3.220	0.200
4	09:04:42.053	09:06:02.657	80.673	281.507	0.043	2.421	3.220	0.200
5	09:07:18.906	09:08:47.791	88.951	370.458	0.040	2.797	3.220	0.200
6	09:10:02.809	09:11:40.764	97.914	468.372	0.042	3.139	3.220	0.200
7	09:12:56.232	09:14:44.125	107.796	576.168	0.046	3.492	3.220	0.200
8	09:16:09.210	09:18:08.072	118.710	694.878	0.044	3.801	3.220	0.200
9	09:19:23.094	09:21:33.681	130.553	825.431	0.045	4.033	3.220	0.200
10	09:22:51.612	09:25:15.420	143.776	969.207	0.043	4.200	3.220	0.200
11	09:26:33.123	09:29:11.116	157.923	1127.130	0.046	4.304	3.220	0.200
12	09:30:28.263	09:33:21.682	173.350	1300.480	0.043	4.391	3.220	0.200
13	09:34:47.780	09:37:59.546	191.562	1492.042	0.048	4.434	3.220	0.200
14	09:39:18.593	09:42:49.592	210.963	1703.005	0.044	4.443	3.220	0.200
15	09:44:12.686	09:48:04.330	231.549	1934.554	0.039	4.458	3.220	0.200

Cyclization: dA^{PhtBu}

#1 Protocol QYDS measurement
#2 Date: 12/10/2020
#3 Sample: dA_Ph_tBu_300nm
#4 Researcher: Simon
#5 LED: 4 NIKKISO VPC1A1 300 nm
#6 Filter::
#7 Solar Cell: HV-00X
#8 Voltage after reference cuvette (V): X.XX, High Power range (A)
#9 Calibration Factor (mW/V): 0.374
#10 Power after reference cuvette (mW): 0.922
#11 Insert comments below, do not change the header up to here

Number	TimeStart	TimeEnd	Runtime	Illum.-Time	Power(mW)	Cell (mW)	Voltage(V)	Current(A)
0	10:45:59.829	10:45:59.829	0.000	0.000	0.000	0.032	0.000	0.000
1	11:10:11.561	11:11:13.168	61.667	61.667	0.012	0.032	5.440	0.200
2	11:12:27.742	11:13:34.478	66.650	128.317	0.015	0.032	5.440	0.200
3	11:17:11.957	11:18:25.549	73.462	201.779	0.009	0.032	5.440	0.200
4	11:19:45.492	11:21:06.116	80.637	282.416	0.010	0.032	5.440	0.200
5	11:22:20.699	11:23:49.692	88.947	371.363	0.014	0.032	5.440	0.200
6	11:25:08.089	11:26:45.920	97.797	469.160	0.013	0.034	5.430	0.200
7	11:28:05.198	11:29:52.988	107.818	576.978	0.009	0.036	5.430	0.200
8	11:31:06.435	11:33:04.615	118.039	695.017	0.012	0.038	5.430	0.200
9	11:34:40.990	11:36:51.675	130.628	825.645	0.013	0.042	5.430	0.200
10	11:38:08.488	11:40:32.373	143.947	969.592	0.014	0.045	5.430	0.200
11	11:41:50.409	11:44:28.275	157.931	1127.523	0.014	0.046	5.430	0.200
12	11:45:45.639	11:48:39.383	173.714	1301.237	0.011	0.047	5.430	0.200
13	11:49:58.197	11:53:10.164	191.899	1493.136	0.012	0.047	5.430	0.200
14	11:54:28.199	11:58:00.322	211.944	1705.080	0.009	0.048	5.430	0.200
15	11:59:13.558	12:03:42.464	268.850	1973.930	0.008	0.049	5.430	0.200
16	12:05:02.960	12:10:00.465	297.427	2271.357	0.005	0.049	5.430	0.200
17	12:11:30.126	12:16:26.064	295.848	2567.205	0.001	0.049	5.430	0.200

Cycloreversion: dA^{PhtBu}

#1 Protocol QYDS measurement
#2 Date: 12/9/2020
#3 Sample: dA_Ph_tBu_CO
#4 Researcher: Simon
#5 LED: 13 OSRAM LVCK7P-JYKZ 508 nm
#6 Filter:: OD1
#7 Solar Cell: HV-00X
#8 Voltage after reference cuvette (V): X.XX, High Power range (A)
#9 Calibration Factor (mW/V): 0.132
#10 Power after reference cuvette (mW): 2.945
#11 Insert comments below, do not change the header up to here

Number	TimeStart	TimeEnd	Runtime	Illum.-Time	Power(mW)	Cell (mW)	Voltage(V)	Current(A)
0	11:09:20.638	11:09:20.638	0.000	0.000	0.000	0.488	0.000	0.000
1	12:51:47.158	12:52:47.845	60.665	60.665	-0.017	0.665	3.110	0.099
2	12:54:07.583	12:55:14.206	66.663	127.328	-0.017	0.842	3.110	0.099
3	12:56:33.438	12:57:47.036	73.651	200.979	-0.015	1.079	3.110	0.099
4	13:07:47.483	13:09:08.335	80.797	281.776	-0.026	1.364	3.110	0.099
5	13:10:32.578	13:12:00.638	87.943	369.719	-0.023	1.693	3.110	0.099
6	13:13:22.276	13:15:00.080	97.687	467.406	-0.024	2.024	3.110	0.099
7	13:16:19.923	13:18:07.708	107.679	575.085	-0.026	2.319	3.110	0.099
8	13:19:27.891	13:21:26.666	118.633	693.718	-0.022	2.560	3.110	0.099
9	13:22:44.398	13:24:55.186	130.565	824.283	-0.021	2.717	3.110	0.099
10	13:26:16.632	13:28:40.887	144.210	968.493	-0.020	2.813	3.110	0.099
11	13:29:59.963	13:32:37.887	157.852	1126.345	-0.022	2.873	3.110	0.099
12	13:33:57.871	13:36:52.184	174.170	1300.515	-0.019	2.897	3.110	0.099
13	13:38:12.941	13:41:25.151	192.141	1492.656	-0.022	2.901	3.110	0.099

Acknowledgements

The authors thank B. Bühler for supplying TMR-DN. We acknowledge H. Rudy, D. Wolf and T. Timmermann (all Heidelberg University) for technical assistance. We also acknowledge H. Derondeau (LMU Munich) for advice on calculating the quantum yields.

Supporting References:

1 W. C. Still, M. Kahn and A. Mitra, *J. Org. Chem.*, 1978, **43**, 2923–2925.

2 F. Gillanders, L. Giordano, S. A. Díaz, T. M. Jovin and E. A. Jares-Erijman, *Photochem. Photobiol. Sci.*, 2014, **13**, 603–612.

3 U. Megerle, R. Lechner, B. König and E. Riedle, *Photochem. Photobiol. Sci.*, 2010, **9**, 1400–1406.

4 H. Volfova, Q. Hu and E. Riedle, *EPA Newsl.*, 2019, 51–69.

5 H. Cahová and A. Jäschke, *Angew. Chem. Int. Ed.*, 2013, **52**, 3186–3190.

6 T. Kolmar, S. M. Büllmann, C. Sarter, K. Höfer and A. Jäschke, *Angew. Chemie Int. Ed.*, 2021, 2–12.

7 L. Dudycz, R. Stolarski, R. Pless and D. Shugar, *Z. Naturforsch.*, 1979, **34**, 359–373.